Title

Adapting and facilitating responses in mouse somatosensory cortex are dynamic and shaped by experience

Journal

Current Biology, 34(15)

ISSN

0960-9822

Authors

Dobler, Zoë
Suresh, Anand
Chari, Trishala
et al.

Publication Date

2024-07-01

DOI

10.1016/j.cub.2024.06.070

Adapting and facilitating responses in mouse somatosensory cortex are dynamic and shaped by experience.

Zoë Dobler[1,2,*], Anand Suresh[1,*], Trishala Chari[1,2], Supriya Mula[1], Anne Tran[1], Dean V. Buonomano[3,4], and Carlos Portera-Cailliau[1,3,‡]

[1]Department of Neurology

[2]Neuroscience Interdepartmental Program

[3]Department of Neurobiology

[4]Department of Psychology

David Geffen School of Medicine at the University of California Los Angeles

Los Angeles, CA 90095

*Zoë Dobler and Anand Suresh contributed equally

‡ Corresponding author: cpcailliau@mednet.ucla.edu; 710 Westwood Plaza, Los Angeles, CA 90095

Key words: 2-photon, barrel cortex, calcium imaging, habituation, population drift, sensitization, stimulus-specific adaptation, whisker.

Abbreviations: 2-photon calcium imaging: 2PCI; AI: adaptation index; FOV: field of view; i.s.i.: interstimulus interval; L: layer; MoM: mean of means; P: postnatal day; ROI: region pf interest; S1BF: barrel field of primary somatosensory cortex;

SUMMARY

Sensory adaptation is the process whereby brain circuits adjust neuronal activity in response to redundant sensory stimuli. While sensory adaptation has been extensively studied for individual neurons on timescales of tens of milliseconds to a few seconds, little is known about it over longer timescales or at the population level. We investigated population-level adaptation in the barrel field of the mouse somatosensory cortex (S1BF) using in vivo 2-photon calcium imaging and Neuropixels recordings in awake mice. Amongst stimulus-responsive neurons we found both adapting and facilitating neurons, which decreased or increased their firing, respectively, with repetitive whisker stimulation. The former outnumbered the latter by 2:1 in layers 2/3 and 4, so the overall population response of mouse S1BF was slightly adapting. We also discovered that population adaptation to one stimulus frequency (5 Hz) does not necessarily generalize to a different frequency (12.5 Hz). Moreover, responses of individual neurons to repeated rounds of stimulation over tens of minutes were strikingly heterogeneous and stochastic, such that their adapting or facilitating response profile was not stable across time. Such representational drift was particularly striking when recording longitudinally across 8-9 days, as adaptation profiles of most whisker-responsive neurons changed drastically from one day to the next. Remarkably, repeated exposure to a familiar stimulus paradoxically shifted the population away from strong adaptation and toward facilitation. Thus, the adapting vs. facilitating response profile of S1BF neurons is not a fixed property of neurons, but rather highly dynamic feature that is shaped by sensory experience across days.

INTRODUCTION

To construct a stable and coherent representation of the external world, sensory circuits must adapt their activity based on the statistics of the surrounding environment. Stimulus-specific sensory adaptation of neuronal activity is a ubiquitous phenomenon across species and sensory modalities, in which the responsiveness of neurons to sensory stimuli is repeatedly adjusted based on the spatiotemporal context in which such stimuli are encountered.[1,2] This is thought to promote the efficient encoding of stimuli in dynamic sensory environments[3-5] by constantly recalibrating neuronal output to maximize the information encoded about external stimuli.[6] Several functions for adaptation have been proposed, including coding efficiency and enhancement of discrimination between stimuli[7] — though at the expense of stimulus detection[8] — and predictive coding.[9,10] Loss of sensory adaptation could make it difficult to ignore certain sensory stimuli and, as such, has been implicated in sensory hypersensitivity symptoms observed in neurodevelopmental conditions.[11-13] For example, adaptation to auditory and tactile stimuli is significantly reduced in humans with Fragile X Syndrome,[14,15] as well as in the *Fmr1* knockout mouse model of FXS.[16,17]

Prior studies have investigated sensory adaptation in different brain regions and animal species, but with certain limitations. It has mainly been studied in single neurons (not across a large population), in acute slices or under anesthesia (less often in awake animals), and at a single time point (not longitudinally over several days).[18-23] Typically, repeated presentation of the same stimulus results in a progressive decrease in neuronal activity.[24] However, facilitating neurons that progressively increase their response magnitude with repetitive stimulation have also been identified in the visual,[25,26] auditory,[27] and somatosensory cortices.[23] This diversity of responses merits further exploration, as it implies that complex population dynamics could occur beyond a net reduction in neuronal response magnitude to a familiar stimulus. At present, it remains unclear how sensory adaptation shapes the activity of neuronal populations and

influences the network-level representation of sensory stimuli. Furthermore, though it may be reasonable to assume that the adaptation profile of individual neurons is stable over time, whether population drift[28] applies to sensory adaptation is not known.

Here, we employed in vivo 2-photon calcium imaging (2PCI)[29] and Neuropixels recordings[30] in excitatory neurons of the barrel field of the somatosensory cortex (S1BF) in awake adult mice to characterize sensory adaptation to vibrotactile stimuli delivered to whiskers. We asked the following questions: 1. Are both adapting and facilitating responses observed in excitatory neurons in S1BF? 2. Is the population adaptation response to one stimulus maintained for a different stimulus? 3. Are adaptation response dynamics stable across tens of minutes and/or across days, or is there representational drift? 4. Does adaptation differ between Layer (L) 2/3 and L4? Our findings support a novel model of sensory adaptation in which neuronal responses are dynamic and experience can reshape population adaptation dynamics across days.

RESULTS

Individual responses of L2/3 excitatory neurons to repetitive whisker stimulation are stochastic, but the population response is adapting.

We first performed in vivo 2PCI to record responses of L2/3 excitatory neurons in S1BF to whisker stimulation in a cohort of young adult (2-3 months) (n=8). We used Slc17a7 (vGlut1)-Cre;GCaMP6s$^{fl/fl}$ (Ai162) mice, in which GCaMP6s expression is restricted to excitatory neurons (see Methods).[31,32] Awake 2PCI was performed while mice were head-fixed and their bodies gently restrained in a plexiglass tube and we used a comb of thin Nylon filaments coupled to a piezo-actuator to deflect most whiskers on one side of the snout in the anterior-posterior axis (see Methods) (**Figure 1A**). Because mice typically whisk spontaneously at frequencies of 5-15 Hz,

and with intermittent bouts lasting 1-4 s,[33] we delivered whisker stimuli at a frequency of either 5 Hz or 12.5 Hz, with a stimulus duration of 1 s and an interstimulus interval (i.s.i.) of 3 s, as in previous studies.[16,17] Before 2PCI, intrinsic signal imaging was performed while stimulating the C2 whisker to identify the C2 barrel in each mouse (**Figure 1B**), which was where calcium imaging was performed. On average, we captured the activity of 159 neuronal somata (range: 67-226 somata) in a single field of view (FOV) (**Figure 1C**).

To determine whether neurons responded reliably to bouts of whisker stimulation, we used either visual inspection of all the traces aligned to the bouts of stimulation, or an automated bootstrapping algorithm we used previously (See Methods; **Figure S1A-B)**.[16] The automated approach tended to miss neurons with a lot of activity just before and/or just after whisker stimulation bouts, whereas the visual inspection method tended to overlook neurons with very small responses to whisker stimulation or those that fired during only a single bout of whisker stimulation (**Figure S1A)**. We opted for the visually selected for all subsequent analyses of 2PCI data. As previously reported most L2/3 neurons in S1BF did not respond to whisker stimulation (**Figure S1C**).[16,34] A slightly larger percentage of stimulus-responsive neurons responded to 12.5 Hz whisker stimulation than to 5 Hz stimulation (19.2 ± 10.0% for 5 Hz vs. 24.5 ± 6.3% for 12.5 Hz, p=0.133, paired t-test; **Figure S1C**). Individual neuronal responses to a sequence of 20 bouts of whisker stimulations at 5 Hz were very variable, with some responding to most bouts of whisker stimulation, while others responded to only a subset of stimulations **(Figure 1C**; see also **Figure S2A)**. Most whisker-responsive neurons (82%) responded to more than half of the bouts (**Figure S2B**). Traces of neurons that were categorized as non-stimulus responsive clearly did not show evidence of whisker evoked activity (**Figure S2C-D**).

At the population level, the mean response in each mouse tended to show adaptation— that is, a gradual decrease in response magnitude with ongoing bouts of stimulation (**Figure 1D**). Together, these data indicate that, despite the stochasticity of individual neuronal responses, the mean response of the L2/3 population in S1BF is adapting, consistent with previous reports.[16,35,36]

Individual L2/3 neurons exhibit adapting and facilitating responses to repetitive whisker stimulation.

If the population response in L2/3 of S1 to repetitive whisker stimulation is adapting, does that mean that individual neurons respond similarly to these stimuli (i.e., do they all adapt)? We found that neuronal responses varied substantially, and not all neurons showed adaptation (**Figure 1C**). Previous studies had reported that some cortical neurons show facilitation, that is, their response magnitudes progressively increase with ongoing stimulation, typically when the i.s.i. is short.[23,25-27,37] We wondered if S1BF neurons can show facilitating responses to repetitive stimulation over tens of seconds, when the i.s.i. is longer.

To categorize stimulus-responsive neurons as either adapting or facilitating (or neither), we calculated a stringent adaptation index (AI) based on whether the slope of the peak responses of individual neurons to the first 15 bouts significantly differed from zero (**Figure 1E**; see Methods). A negative AI value indicates an adapting response profile, while a positive AI value denotes facilitation (see examples in **Figure 1F**). Together, facilitating (7.2%) and adapting neurons (18.6%) comprised roughly a quarter of all responsive neurons; the remainder showed non-significant AI slope values (**Figure 1G**). Within this non-significant category, some cells could show adaptation or facilitation, but due to variable responses across the 15 stimulations, our strict AI criteria did not assign as either facilitating or adapting. To assess the population response, we plotted the mean activity of all adapting or facilitating neurons from each mouse and computed a "mean of means" (MoM) trace. This MoM trace for all adapting and facilitating neurons across all mice showed the expected trajectories (**Figure 1H**).

We also used a different approach to classify L2/3 neurons as adapting or facilitating based on the change in magnitude of the response peaks from stimulations 1-5 to stimulations 11-15 (**Figure S3A-B**) (see Methods). This alternate approach identified comparable proportions

of adapting (25.4%) vs. facilitating neurons (12.7%) in L2/3 (**Figure S3C**), and their respective MoM traces resembled those of our more stringent statistical method (**Figure S3D**). Thus, regardless of the method we used to quantify the AI, neurons with adapting responses outnumbered those showing facilitation by ~2:1.

When we superimposed all FOVs (each approximately centered above the C2 barrel), we found a salt-and-pepper distribution of adapting and facilitating neurons, and no evidence of spatial segregation (**Figure 1I**). During the pre-stimulus baseline, adapting neurons were more correlated to each other than to facilitating neurons (**Figure 1J**, left). During stimulation, correlation coefficients were significantly higher for adapting-adapting and facilitating-facilitating pairs than for adapting-facilitating pairs (**Figure 1J**, right), but this was likely due to their preferential firing during early or late bouts of stimulation, respectively (**Figure 1K**).

We also analyzed neuronal responses and sensory adaptation profiles to 12.5 Hz whisker stimulation in the same animals (**Figure S3E**). The relative proportion of adapting and facilitating neurons were similar (14.4% vs. 12.0 %, respectively; **Figure S3F**). Thus, although the percentage of adapting neurons was similar between 5 Hz and 12.5 Hz stimulation on average across mice, the percentage of facilitating neurons was significantly higher with 12.5 Hz stimulation (**Figure S3G**). As a result, the mean significant slope of all responsive neurons was significantly less negative (less adapting) for 12.5 Hz compared to 5 Hz stimulation (**Figure S3H**). This was the first hint that adaptation is dynamic at the population level.

Adaptation profiles at higher frequencies and for single whisker stimulation

Although mice naturally whisk at 5-15 Hz, previous studies had also investigated adaptation at much higher frequencies of whisker stimulation.[23] In a separate cohort of mice (n=5), we also examined responses in S1BF to 25 Hz and 50 Hz. Perhaps not surprisingly, compared to 5 Hz stimulation (**Figure 1G**), we found higher proportions of adapting (24.4% and 33.6% for 25 Hz and 50 Hz, respectively) and slightly smaller proportions of facilitating neurons (3.3% and 7.5%

for 25 Hz and 50 Hz, respectively; **Figure S4A**). The MoM trace for these mice tended to reflect this higher adaptation (**Figure S4B**).

Because multi-whisker stimulation strongly activates inhibition it could lead to exaggerated adaptation, as neurons within a given barrel are inhibited by stimulation of surround whiskers.[38] To address this possibility, we tested whether responses might be different during single whisker stimulation.[39] In the same cohort of mice in which we tested higher frequencies, we trimmed all the whiskers except C2 and performed in vivo 2PCI again but stimulated only the spared C2 whisker. We found that the percentage of whisker-responsive neurons in S1BF was slightly lower for single whisker stimulation compared to multi-whisker stimulation across all frequencies, but higher frequencies of stimulation still recruited more neurons (**Figure S4C**). The proportion of adapting and facilitating cells was similar for single whisker stimulation (22.7% and 9.1%, respectively; **Figure S4D**) and multi-whisker stimulation (18.6% and 7.2%, respectively; **Figure 1G)**. Overall, the mean significant slope was not different between single whisker and multi-whisker stimulation, but it more adaptation at higher frequencies (**Figure S4E**).

State of arousal

We considered the possibility that adaptation might be related to state of arousal of the animal.[24] For instance, mice might be hyper-aroused during the first few bouts of whisker deflections because of the unexpected surprise of the stimulation, but then gradually habituate. Therefore, we used a video camera aimed at the face of the mouse and FaceMap[40] (**Figure S5A-B**; see Methods) to track pupil size in the subset of mice stimulated at higher frequencies (n=5). Pupil size gradually grew over the course of 20 bouts of whisker stimulation, but only by <50% (**Figure S5C**). Within individual bouts, the pupil also enlarged slightly, but there was substantial variability from bout to bout (**Figure S5D**). When we overlaid the MoM trace of neural activity across all bouts of whisker stimulation, we observed that adaptation occurred quickly, after only a few bouts, whereas pupil dilation developed more gradually (**Figure S5E**). This hyperarousal

perhaps reflects the slightly aversive nature of ongoing whisker stimulation. On the other hand, we did not observe wide fluctuations in pupil size before each round of stimulation that could explain differences in neural activity (**Figure S5F**). In one animal the pupil was much larger than in the others, and its L2/3 neurons in S1BF showed slightly more adaptation (**Figure S5F-H)**. We also found that the response of L2/3 neurons to the first whisker stimulation did not change significantly across different rounds of stimulation and did not appear to correlate with the degree of adaptation (**Figure S5I-J)**. Finally, we wondered whether the magnitude of neuronal activity during the baseline period immediately before the first whisker stimulation might influence the adaptation profile of each cell. However, we found no significant correlation between the mean z-score of stimulus-responsive neurons during the 20 s baseline and the slope of the adaptation index for the same cells (**Figure S5K**).

Neuropixels recordings confirm the presence of adapting and facilitating neurons in L2/3 of S1BF

The slow temporal resolution of 2PCI[29] could contribute to an overestimation of facilitating responses if the fluorescence intensity did not fully return to baseline prior to the next stimulation (particularly in highly active cells). Although we have observed this phenomenon when using bouts of whisker stimulation with a shorter i.s.i. of 1 s (not shown), we did not observe a significant additive profiles of calcium transients using a 3 s i.s.i.. GCaMP6s imaging might also have missed neurons that responded with few action potentials. To address this, we performed in vivo electrophysiological recordings in S1BF with Neuropixels probes[30] (see Methods; **Figure 2A-B**) in a new cohort of mice (n=9) presented with 20 bouts of whisker stimulation at 10 Hz. Our analysis focused on regular-spiking excitatory neurons across all cortical layers (579 single units). Again, we calculated an AI for stimulus-responsive neurons based (**Figure 2C**), which revealed both adapting and facilitating neurons with stochastic response profiles to individual bouts of stimulation, just as we had observed with 2PCI (**Figure 2D**). The relative proportions of adapting

(25.0%) and facilitating neurons (6.3%), as well as the mean traces of adapting and facilitating neurons, were similar between Neuropixels recordings and 2PCI (**Figure 2E-F**).

Adapting neurons transiently facilitate after a switch to whisker stimulation at a higher frequency.

Is the adapting or facilitating identity of a neuron in S1BF fixed? And, at the population level, can the overall response in S1BF change with different stimulation parameters or with experience? To begin to answer these questions we first considered whether cortical neurons maintain the same sensory adaptation identity after a switch in stimulation parameters (i.e., do S1BF neurons that adapt to repetitive whisker stimulation at one frequency also adapt to a different frequency?). We performed frequency switch experiments, in which we delivered 10 stimulation bouts (1 s duration, 3 s i.s.i.) at one frequency (5 or 12.5 Hz) and then abruptly switched to the alternate frequency for the next 10 stimulation bouts (**Figure 3A**). As a control, the same mice were stimulated at the same frequency for all 20 stimulation bouts. During the control paradigms, the mean population response of all whisker-responsive neurons progressively decreased, as expected, regardless of frequency, though slightly more so with the higher frequency (**Figure 3B**).

We then classified neurons as adapting or facilitating by calculating the AI based on the slope of peak responses to the first 9 stimulations. We found that facilitating neurons did not exhibit any substantial change in response peak amplitudes after the frequency switch compared to the control stimulation (**Figure 3C-F,** bottom). In contrast, adapting neurons exhibited a noticeable increase in their response peak amplitudes after a switch to the higher frequency (**Figure 3C-F**, top). Of note, the increase in response peak amplitude of adapting neurons was not due to an 'oddball' phenomenon, as it did not occur immediately after the switch but rather emerged

gradually because of facilitation (**Figure 3C-D**). When we quantified the difference in mean peak z-score before and after the switch, we found that adapting neurons exhibited a significant change, which was not seen in the control protocol (**Figure 3E-F, top**). In contrast, facilitating neurons did not manifest a significant change in the mean peak z-score (**Figure 3E-F**, bottom), and neither did neurons with non-significant AI (**Figure S6A-B**). Moreover, a change in response peak amplitudes was not observed for adapting or facilitating neurons when switching to a lower frequency (**Figure S6C-D**). Normalizing peak Z scores to the first response peak showed similar results for the upward frequency switch (not shown).

We also used Neuropixels probes to record responses during the same frequency switch experiment. These recordings confirmed that adapting neurons significantly increase their firing (i.e., they become facilitating) in response to a switch to a higher frequency, whereas facilitating neurons do not (**Figure 3G-H**). Altogether, frequency-switch experiments revealed that, although most stimulus-responsive L2/3 neurons appear to maintain the same dynamics following a sudden switch in stimulus frequency, adapting neurons can gradually increase their activity in response to an increase in frequency, in essence exhibiting facilitation.

During these experiments, the adaptation profile of L2/3 neurons (adapting, facilitating etc.) was remarkably dynamic. Most neurons that adapted or facilitated during the control paradigm did not maintain the same response profile during the switch paradigm (**Figure S7A**). Thus, neurons categorized as adapting in the control paradigm and those categorized as adapting in the frequency-switch paradigm were not necessarily the same neurons. To account for this, we also plotted MoM traces with the same subset of neurons for both the control and switch paradigm, such that the MoM traces were comprised only of cells that adapted or facilitated during the control protocol (**Figure S7B**). When plotting the MoM traces using only those cells and quantifying these results, we did not observe an increase in the response peak amplitude for initially adapting cells after the upward frequency switch (**Figure S7C**). Therefore, the sensitivity of whisker-responsive

neurons to an upward frequency switch (as observed in **Figure 3C-F**) depends on how they respond during the initial stimulations of the current paradigm.

The adaptation profile of individual L2/3 neurons is highly dynamic across tens of minutes, but the population maintains a stable proportion of stimulus-responsive neurons.

Given the heterogenous response profiles of individual neurons within L2/3 of S1BF, and the fact that their adaptation profile was highly dynamic during the frequency switch experiments, we next asked how stable the population is across a time scale of tens of minutes. We repeated our 5 Hz stimulation protocol (20 bouts) six times (rounds R1-R6) every 4-5 min, while longitudinally recording the same L2/3 neurons with 2PCI in 6 mice (**Figure 4A-B**). While the proportion of neurons responding to whisker stimulation on any given round remained stable on average (**Figure 4C**, left), the specific neurons that responded to whisker stimulation changed from one round to the next. Across successive rounds of stimulation, the cumulative percentage of stimulus-responsive neurons increased significantly (**Figure 4C**, right). This highlights how individual neurons are stochastic in their whisker responsiveness and yet, at the population level, a stable proportion of L2/3 neurons (~20%) is available to respond. As one might predict, with ongoing rounds of whisker stimulation, the population became slightly more adapting (**Figure 4D**) because of a slight decrease in the proportion of facilitating neurons (**Figure 4E, right**), though these trends were not significant.

L2/3 neurons were seemingly stochastic in their adaptation profiles across different rounds of whisker stimulation, for example showing clear adaptation for one round of whisker stimulation then becoming non-responsive or even adapting on a subsequent round (**Figure 4F-G, Figure S8A**). The overall range of adapting and facilitating response profiles (ordered according to AI values) remained unchanged from R1 to R5 (roughly 40 min apart), albeit in a largely different

subset of neurons (**Figure 4G**). Although many neurons exhibited highly capricious adaptation profiles, few cells drastically switched their identity from adapting to facilitating (or vice versa). Instead, most neurons exhibited either no change or mild changes in response profile (**Figure S8B**; e.g., nonsignificant → adapting/facilitating or vice versa). The change in adaptation profile from one round of stimulation to the next was not entirely stochastic, as neurons in any category (adapting or facilitating) tended to remain in that category (**Figure 4G**). Indeed, the correlation between adaptation index values of the same neurons on R1 and R3 was higher than on R1 and R5 (**Figure 4H**) This gradual shift in adaptation profiles is consistent with population drift, rather than a completely stochastic process. Together, these results indicate that L2/3 maintains a stable proportion of stimulus-responsive neurons across tens of minutes, even though their responsivity and adaptation profile can change drastically. Although rare neurons will switch between facilitating and adapting response profiles, most do not, and over multiple rounds of whisker stimulation, the population trends slightly toward more adaptation.

Representational drift of adapting/facilitating neurons in L2/3 across several days.

Our results above indicate that the encoding of whisker stimulation in L2/3 exhibits remarkable population drift even within a single imaging session (<1 h). We next investigated whether sensory adaptation dynamics might also change due to sensory experience across days. We conducted 2PCI in the same FOVs in individual mice (n=8) across 4 separate imaging sessions spanning 8-9 days (**Figure 5A**), recording L2/3 excitatory neuron responses to 20 stimulations at 5 Hz. We identified the same active L2/3 neurons shared between Day 1 and subsequent sessions using the probabilistic cell-tracking method *CellReg* [41] (**Figure 5B**).

We observed remarkably diverse responses of the same identified neurons to 20 whisker stimulation bouts across daily imaging sessions (**Figure 5C**). Cells that responded to only a few

bouts of whisker stimulation on one day could respond to most bouts on a different day, and vice versa. The proportion of stimulus-responsive neurons remained stable across days (**Figure 5D**). We then asked whether this sensory experience across days affected sensory adaptation at the population level. To gain a more nuanced understanding of the adaptation profile of the L2/3 population across days, we further divided adapting and facilitating neurons into weak and strong subcategories based on their slope value (see Methods). The proportion of stimulus-responsive neurons categorized as nonsignificant remained relatively stable across days (**Figure 5E**). Unexpectedly, however, we observed a decrease in the proportion of strongly adapting neurons, coupled with an increase in weakly adapting and weakly facilitating neurons (**Figure 5E**). This resulted in a significant increase in the mean significant AI slope for neurons across days from Day 1 to Day 8/9 (**Figure 5F**). Thus, experiencing the same whisker stimulation protocol repeatedly across several days caused a progressive population-level shift toward a less adapting profile.

When focusing only on a subset of neurons that we successfully tracked longitudinally across multiple days (220/1,269 cells that were tracked on Days 1 and 2; 120/917 cells tracked on Days 1 and 8/9), we confirmed that most of them did not maintain the same response profile, though most non-responsive (86.0%) neurons remained so from Day 1 to Day 8/9 (**Figure 5G**). When comparing Day 1 to Day 8/9, most tracked stimulus-responsive neurons exhibited a change in response profile, including 17.4 ± 8.0 % of neurons exhibiting a mild change in adaptation identity (e.g., NS→A, F→NS), and over 50% becoming nonresponsive (**Figure 5H**, green). Importantly, no neurons exhibited a major change (A→F or F→A) from Day 1 to Day 8/9, and 27.4 ± 3.6% of whisker-responsive cells maintained their adaptation identity after 1 week. Across all imaging days, major changes were rare, and ~10% of cells tracked on at least 2 days exhibited a mild change (**Figure S8C**).

Great care was used to ensure that the positioning of the comb of filaments used for stimulation was positioned in a way that whiskers would be deflected consistently across days.

To confirm that the positioning of the stimulator relative to individual whiskerswas similar across days, we used a video camera to record the deflections of whiskers in a subset of mice and DeepLabCut[42] to track the displacement of individuals whiskers (see Methods). This analysis revealed that, across sessions from Day 1 to Day 8, whiskers were reliably deflected in a consistent manner (**Figure S9**).

L4 exhibits distinct but similar longitudinal population dynamics compared to L2/3.

The adaptation and facilitation profiles of L2/3 neurons could emerge from local computations in L2/3, or they could be inherited from upstream circuits, such as L4 or the thalamus. L4 is the primary recipient of thalamocortical inputs[43] and could inherit a strong adapting response profile from the thalamus. Alternatively, as the superficial layers are the major recipients of projections from other cortical areas,[44,45] L4 could exhibit less adaptation because it is not subject to as much top-down modulation as L2/3. To further investigate this, we repeated the longitudinal imaging protocol in Scnn1a-Cre;GCaMP6s$^{fl/fl}$ mice to characterize the response dynamics of L4 spiny stellate neurons over several days (**Figure 6A**). Just as in L2/3, the overall response of the L4 population was slightly adapting in individual mice (**Figure S10A**). L4 neurons tended to respond to fewer bouts of whisker stimulation than to those in L2/3 (**Figure 6B; Figure S10B**), and the average proportion of stimulus-responsive neurons in L4 was even lower than in L2/3 (**Figure 6C**), consistent with recent findings.[46]

Longitudinal imaging across 8 days revealed that the L4 population showed a decrease in the proportion of weakly adapting neurons and an increase in the proportion of strongly facilitating neurons (**Figure 6D**), which we had not observed in L2/3. Nevertheless, L4 neurons also showed a slight increase in the mean significant slope of the adaptation index (**Figure 6E**), similar to what we had observed in L2/3. Although this trend was not statistically significant in L4 (there was more variability and a smaller sample size), the overall effect of experience was similar across

both layers. Moreover, L4 neurons tracked across multiple days also exhibited substantial drift, changing their response profiles (**Figure 6F-G**). The proportion of neurons exhibiting a mild change in response profile was markedly larger between Days 1 and 8 compared to Days 1 and 2 (6.7 ± 9.9% between Days 1 and 2 vs. 35 ± 38.4% between Days 1 and 8) (**Figure 6G**), while this proportion had remained relatively stable in L2/3 (14.9 ± 8.6% between Days 1 and 2 vs. 17.4 ± 8.1% between Days 1 and 8/9). When looking across all imaging days and assessing all stimulus-responsive neurons tracked on at least 2 days, mild changes comprised a small fraction of cells (3.1%, **Figure S10C**). Together, these results suggest that individual L4 neurons exhibit dynamic shifts in their response profiles, but they show similar experience-dependent plasticity of sensory adaptation at the population level as L2/3.

Thalamocortical boutons exhibit larger degree of sensory adaptation.

Finally, we investigated sensory adaptation in thalamocortical axons projecting to L4 of S1BF acutely in anesthetized mice (n=5). We injected a rAAV virus to express GCaMP6s in the ventral postero-medial (VPM) nucleus of the thalamus at the time of the cranial window surgery (see Methods, **Figure S11A**) and recorded calcium transients of individual boutons within L4 of S1BF during bouts of whisker stimulation at 5 Hz (**Figure S11B**). One-third of thalamic boutons responded to whisker stimulation (33% ± 9%, **Figure S11C**). The MoM trace for all mice showed prominent adaptation (**Figure S11D**). Like cortical neurons, individual boutons showed adapting and facilitating responses (**Figure S11E**). The proportion of boutons showing adapting responses was much higher than that of boutons showing facilitation (39% vs. 5%, **Figure S11F-G**).

DISCUSSION

Beyond its important roles in sensory discrimination and predictive coding, sensory adaptation is critical for tuning out repetitive, non-threatening or non-salient, familiar/redundant stimuli across

sensory modalities.[3,6,8,47] Most of this evidence has come from studies in single neurons across fast time scales (a few seconds or less). This motivated our study to investigate adaptation at the neuronal and population level and across longer times scales (minutes to days). Our principal goal was to determine whether the temporal profile of neuronal responses to repetitive stimuli was fixed or plastic over these time scales, and whether it could change based on experience. Using 2PCI and Neuropixels recordings in S1BF of awake mice we characterized adaptation dynamics in hundreds of excitatory neurons in L2/3 and L4, and in thalamocortical axon boutons. We found that: 1) The mean population response of excitatory cortical neurons to repetitive stimuli is mildly adapting; 2) Individual neurons exhibit a wide array of sensory adaptation response profiles, ranging from strongly facilitating to strongly adapting; 3) The adaptation profile of L2/3 neurons to one stimulus can change for different stimulus frequencies (neurons that adapt to bouts of 5 Hz whisker stimulation can exhibit facilitation to 12.5 Hz); 4) S1BF populations show dramatic drift in their responses to whisker stimuli and in the adaptation profile over just a few minutes; and 5) Despite this stochasticity, sensory adaptation in L2/3 and L4 can be shaped by experience across days, such that the population becomes less adapting to a familiar stimulus. Thus, in contrast to the standard view that sensory adaptation reflects a hardwired and rigid property of neural responses, our studies suggest that sensory adaptation is plastic and sculpted by experience.

While sensory adaptation is generally thought of as a progressive decrease in neuronal responsiveness with repetitive stimulation, a minority of neurons can show facilitating (or sensitizing) responses. In primary auditory cortex, one study found that ~13% of units exhibited facilitation,[27] while another found only 6%.[37] Similarly, in S1BF, facilitating neurons comprise a small (<10%) fraction of the population.[23,48-50] In our studies ~6-12% of L2/3 neurons showed significant facilitation to repetitive whisker stimuli, regardless of whether we used 2PCI or Neuropixels recordings. Even fewer S1BF neurons showed facilitation when we used higher frequencies of stimulation (25-50 Hz). Although we observed slightly more adapting and

facilitating neurons when stimulating only the C2 whisker, the general characteristics of adaptation were similar to those we observed with multi-whisker stimulation.

A previous study in S1BF reported that input layers like L4 tend to show facilitation while L2/3 shows adaptation.[48] Our data show a different pattern: we observed slightly more adapting neurons in L4, and even greater degree of adaptation in thalamocortical boutons (18.6% in L2/3, 28.3% in L4; 39% in thalamocortical boutons). This discrepancy may be due to the use of different stimulation parameters and conditions.[48]

As is generally the case in sensory adaptation studies, it is important to consider whether the stimulation protocol is likely to reflect naturalistic conditions (e.g., whiskers were passively stimulated). We chose a duration and frequency of stimulation that are within the range of natural whisking (5-15 Hz) and suspected that active object sensing with whiskers would not induce as much adaptation, at least over fast timescales of <2 s.[51] For instance, whisking during a pole detection task produces much more variable amplitudes and rates of whisker deflections.[46,52,53] Nevertheless, future studies that extend our investigations to active whisking during object exploration will undoubtedly add to our understanding of population-level of adaptation.

The method used for classifying responses as either adapting/facilitating could also influence the estimates of their relative abundance. Of note, we found very similar results when using two different methods to calculate the AI, or two methods for recording neuronal activity (2PCI vs. Neuropixels) (**Figures 1G** and **2E**). The linear fit approach we used was based on a published study[37] and is a simple method with relatively few assumptions, yet statistically robust. While it is possible for some neurons to fluctuate between being classified as nonsignificant or as adapting/facilitating, the slope value itself numerically represents each neuron's response profile, with larger values representing steeper increases/decreases in response magnitude over time. This is why we assessed longitudinal changes in adaptation not only by quantifying the percentage of neurons in each category (**Figure 5E**) but also by plotting the mean slope of those significant neurons (**Figure 5F**). And regardless of whether we ultimately classify neurons as

adapting or facilitating, the mean significant slope clearly changes progressively over days with experience.

We also wondered whether the behavioral state of the animal might also dynamically modulate levels of adaptation and facilitation within the population, even if mice remained relatively still during whisker stimulation, with minimal whisking. Previous studies in S1BF have shown that sensory adaptation is sensitive to arousal state, such that sensory responses are already adapted in behaviorally activated states.[24] We found that the pupil became only slightly more dilated with ongoing whisker stimulation, consistent with the notion that stimulation might have been aversive (**Figure S5**). But we did not find wide fluctuations in pupil size across different bouts or rounds of whisker stimulation that could explain the varying responses of individual neurons or the overall adaptation of the population.

By recording neuronal responses during a single session, previous studies might have given the impression that individual neurons are always adapting or facilitating, and that they permanently retain such phenotypes. One of our most striking observations was that adaptation response profiles (adapting vs. facilitating) are not a fixed property of a neuron. Indeed, S1BF neurons can adapt to one stimulation frequency and then facilitate to another frequency or change their adaptation profile across minutes or days. Single-session recordings had previously shown that S1BF neurons that facilitate at certain stimulation frequencies do not necessarily respond in the same way to other frequencies.[54] However, we show the scale of this turnover within a single-day imaging session and across days, and are the first to demonstrate a shift towards facilitation with daily experience of whisker stimulation.

We also report that an abrupt change in stimulus parameters is not encoded equally across all neurons, as only those that had adapted to 5 Hz showed a change in activity to a sudden switch to 12.5 Hz. Thus, adapting neurons may be best poised to represent changes in tactile stimuli as a mouse navigates its environment, which is consistent with the notion that adaptation is useful for detecting deviant stimuli.[47] Importantly, the behavior of adapting neurons after the

frequency switch did not resemble a classic "oddball response"[36,55] because it emerged gradually through evidence accumulation. This gradual readjustment in firing magnitude may reflect an important balance that the network must maintain achieve in a timely and efficient manner, but not too quickly so as to avoid incorrectly recalibrating neuronal responsiveness when a change in the parameters (e.g., frequency) of forthcoming stimuli has not actually occurred.[21]

Previously, population drift had been observed for whisker tuning of L2/3 neurons in S1BF,[56] but to our knowledge, we are the first to demonstrate representational drift of their adaptation profiles (**Figure 4G**). That S1BF neurons gradually became less adapting after several days of whisker stimulation may seem counterintuitive considering the stimuli were neither threatening, nor behaviorally relevant. Because this did not occur after multiple rounds of stimulation within a single imaging session, we surmise that recurrent familiar stimuli occurring infrequently (one daily session) must have gained some salience for the mice that is encoded in the network as facilitation. Future studies that examine the role of facilitation— perhaps using optogenetics to artificially modulate neuronal activity over time or rewards to provide behavioral salience — should explore its role in perception and stimulus representation.

What are the mechanisms responsible for sensory adaptation? At the level of individual neurons, somatic currents and the short-term depression of thalamocortical synapses[2,18] have been implicated in adaptation over fast time scales (tens to hundreds of milliseconds). Interestingly, over the longer time scales of our experiments (over seconds), thalamocortical axon boutons show a significantly higher proportion of adaptation than L4 neurons or L2/3 neurons.[57] We speculate that adaptation is a bottom-up phenomenon that the neocortex inherits from the thalamus, as previously suggested,[58] whereas facilitation (reflecting salience of a stimulus) may require top-down modulation at cortical levels. GABAergic inhibition through different subtypes of interneurons could play a role at the longer time scales we recorded by gradually reducing the firing of excitatory neurons. For example, in the auditory system, fast-spiking parvalbumin interneurons modulate excitatory firing in the same way before and after adaptation, while

somatostatin neurons more strongly inhibit neurons that have strongly adapted.[36] Furthermore, during a single recording session, repetitive whisker stimulation elicits stronger adaptation in inhibitory inputs than excitatory inputs, leading to a net excitatory effect in the network.[59] We examined sensory adaptation in fast-spiking (FS) units (corresponding to putative interneurons) in our Neuropixels recordings (see Methods). Although the sample size was very small (only 22 FS cells in 5 mice were stimulus responsive), we found that the proportion of FS neurons showing adaptation outnumbered 3:1 those showing facilitation (27.3% and 9.1%, respectively; **Figure S12**). However, even though FS interneurons tend to adapt, consistent with prior work,[58] this does not mean that they do not play a role in the overall adapting response of the S1BF population. Future studies that modulate the activity of different interneuron subtypes can test their role in population adaptation/facilitation and whether they contribute to the net facilitatory effect we observed with longitudinal imaging over > 1 week.

In addition, exposure to repetitive sensory stimuli over timescales of tens of seconds likely engages higher-order brain regions to access prior knowledge or expectations regarding the statistics of forthcoming stimuli. Under a predictive coding framework, higher-order areas send predictive signals to primary sensory areas via feedback projections to induce or lessen adaptation, depending on the stimulus.[10,60] Reciprocal connections exist between neurons in L2/3 of S1BF and secondary somatosensory cortex and vibrissal primary motor cortex.[45,61-63] Elucidating the impact of both interneurons and top-down feedback projections on population adaptation will be an important next step in understanding sensory adaptation.

In conclusion, our study revealed remarkably complex dynamics of sensory adaptation across populations of S1BF neurons, which were shaped by experience over days. This experience-dependent plasticity has profound implications regarding the primary function of sensory adaptation. Specifically, if it primarily reflects predictive coding (tuning out an expected stimulus), it is not clear why it would undergo an experience-dependent shift towards facilitation across days. In contrast, if sensory adaptation contributes to the formation of representations that capture the

temporal structure of repeating stimuli, one might expect the observed shift towards facilitation. Future work examining candidate mechanisms underlying population adaptation, as well as the distinct functions of facilitation and adaptation in sensory perception, will provide valuable insights about how it ultimately impacts behavior.

Author contributions: Conceptualization, Z.D, D.V.M., and C.P.-C. Methodology, Z.D., A.S., T.C., S.M., A.T., D.V.M., and C.P.-C. Z.D. and C.P.-C. wrote the manuscript with input from other authors.

Acknowledgements: This work was supported by the following grants: R01NS117597 (NIH-NINDS), R01HD108370 and R01HD054453 (NIH-NICHD), Department of Defense (DOD, 13196175) awarded to C.P-C, Training in Neurotechnology Translation T32NS115753 (NIH), F31HD108043 (NIH/NICHD), a Jessamine Hilliard Neurobiology Graduate Student Grant awarded to Z.D., a graduate student fellowship from the Achievement Rewards for College Scientists Foundation to T.C., Marion Bowen Neurobiology Postdoctoral Fellowship for A.S, a Bennet and Jeanelle Duval Undergraduate Scholarship to S. M., and a Whitcome Fellowship to S.M. We are also grateful to William Zeiger, Nazim Kourdougli, Dario Ringach, Maria Geffen, and Ladan Shams for their helpful conversations.

Declaration of interests: The authors declare no competing interests.

MAIN FIGURE LEGENDS

Figure 1. Adapting responses outweigh facilitating responses in L2/3 of S1BF.

A) Top, cartoon of 2PCI and whisker stimulation setup. Bottom, trajectory of piezoactuator deflections for the 1 s stim duration, 3 s i.s.i. stimulation paradigm. Frequency is 5 or 12.5 Hz.

B) Top, cranial window and superimposed intrinsic signal imaging map (green) corresponding to the C2 barrel in S1BF. Bottom, representative FOV from 2PCI in L2/3 above the C2 barrel (scale bar: 100 μm). M, medial. L, lateral.

C) Example traces of stimulus-responsive (SR) neurons during 5 Hz whisker stimulation.

D) Mean traces of all SR neurons from 4 representative mice during whisker stimulation at 5 Hz. Note that the mean population response is mildly adapting.

E) Calculation of adaptation index. Top, example neuron with response peaks labeled in red. Bottom, linear regression-based calculation of adaptation index in the same example neuron.

F) Traces of 6 example L2/3 neurons from the same movie, showing adapting or facilitating responses to whisker stimulation (5 Hz, 1 s stim, 3 s i.s.i.), with corresponding adaptation index values.

G) Relative proportion of adapting, facilitating, and nonsignificant neurons.

H) MoM traces of all adapting (red) and facilitating (blue) neurons responding to whisker stimulation.

I) Spatial distribution of adapting and facilitating neurons within all FOVs (n=236 cells from 8 mice), approximately aligned to each other with respect to the C2 barrel. M, medial. L, lateral. A, anterior. P, posterior.

J) Left: Mean correlation coefficient for neuron pairs during the 20 s baseline period preceding the first whisker stimulation. Right: Same, but for the stimulation bouts. Kruskal-Wallis test with post-hoc Dunn's test. A: adapting; F: facilitating

K) Mean correlation coefficient of neuron pairs with distinct response profiles during each stimulation bout. Blue: facilitating-facilitating pairs; Red: adapting-adapting pairs; Dashed line: all stimulus-responsive neurons. Solid lines are means, shaded regions are s.e.m.

Figure 2. Neuropixels recordings of regular-spiking neurons in S1BF confirm preponderance of adapting over facilitating neurons after repetitive whisker stimulation.

A) Schematic of Neuropixels recording setup.

B) Example raster plot from one animal during the first 5 whisker stimulations at 5 Hz. Approximate boundaries of cortical layers are noted.

C) Adaptation index calculation in an example regular-spiking (RS) unit.

D) Example adapting and facilitating neurons during 10 Hz whisker stimulation.

E) Relative proportion of adapting, facilitating, and non-significant RS neurons in S1BF.

F) Mean trace of all adapting (red) and facilitating (blue) neurons responding to 10 Hz whisker stimulation.

Figure 3. Adapting neurons transiently facilitate after an upward switch in stimulus frequency.

A) Schematic of control (left) and frequency switch (right) whisker stimulation protocols. Each vertical bar represents a single 1 s-long whisker stimulation at 5 or 12.5 Hz (also shown in expanded timeline).

B) MoM traces for animals presented with the 12.5 Hz (top) and 5 Hz (bottom) control protocols. Gray lines represent mean trace of all stimulus-responsive (SR) neurons for individual mice and thick black lines represent the MoM trace for all animals.

C) MoM traces of adapting (top) and facilitating (bottom) neurons from the same mice in **B** for the downward frequency switch (left) and upward frequency switch (right) protocols. Control traces (red or blue) and switch traces (green) are scaled to the first response peak.

D) Same traces as in **C** but expanded to highlight stimulations 6-15 (the vertical dashed line indicates the frequency switch).

E) Mean peak Z scores of adapting/facilitating neurons at stims 6-10 and 11-15 for the 5 Hz → 12.5 Hz switch protocol and 5 Hz control protocols. Wilcoxon test.

F) Change in mean peak Z score from stims 6-10 to stims 11-15 in the control 5 Hz control protocol vs. the 5 Hz → 12.5 Hz switch protocol, calculated using the following formula: ((Mean Peak Z score stims 11-15) – (Mean Peak Z score stims 6-10))/(Mean Peak Z score stims 6-10). Mann Whitney test (top, non-normal distribution) and unpaired t-test (bottom). Same cells as in **E**.

G) MoM traces of adapting and facilitating neurons during the upward frequency switch protocol using Neuropixels recordings.

H) Same as in **E**, but for Neuropixels recordings. paired t-test (top) and Wilcoxon test (bottom, non-normal distribution). Same cells as in **G**.

Figure 4. The adaptation profile of individual L2/3 neurons is highly dynamic across different rounds of 20 whisker stimulations over tens of minutes.

A) Schematic of repeated stimulation protocol within a single imaging session. Mice are exposed to 6 different rounds of the same whisker stimulation protocol (20 stimulation bouts), with a 4-5 min break between each round.

B) Example FOV (GCaMP6s expression in Slc171a-Cre;Ai162 mice) tracked across 6 rounds of whisker stimulation in a single imaging session.

C) Left, percent of L2/3 neurons responding to whisker stimulation on each round. Kruskal-Wallis test. Right, cumulative percent of neurons responding to whisker stimulation with each round of stimulation. Kruskal Wallis test. (n=908 total neurons imaged across 6 mice).

D) Mean slope value of adaptation index for all neurons with a significant linear regression. (The number of stimulus-responsive neurons with significant AI slope are indicated for each round). Kruskal-Wallis test.

E) Percent of whisker-responsive neurons that adapt (left) or facilitate (right) on each stimulation round. Kruskal Wallis test. Kruskal-Wallis test.

F) Traces of example neurons at different rounds of whisker stimulation. Note the stochasticity of responses (with respect to individual bouts of 5 Hz stimulation) and the dynamic changes in their adaptation profile between different rounds.

G) Left: heatmap of response profiles for all neurons that are stimulus-responsive (SR) in R1, sorted by adaptation index during R1. Top right: heatmap of response profiles for all neurons that are SR in R5, sorted by adaptation index during R5.

H) Left: XY plot of the AI values of SR neurons on R1 (x axis) and R3 (y axis). Spearman correlation coefficient and corresponding p-value are displayed. Right: Same, but for R1 (x-axis) and R5 (y-axis).

Figure 5. Experience-dependent decrease in L2/3 population adaptation across days.

A) We performed longitudinal 2PCI in the same FOV (left) in L2/3 across 8/9 days. Top left: example FOV from Slc171a-Cre;Ai162 mouse (scale bar: 100 μm). Top right: enlarged view of a portion of the FOV (red box).

B) CellReg procedure to identify tracked cells across imaging days. Detected ROIs within the red box (top left) on days 1 and 2 of imaging. Using CellReg, masks of active neurons are then overlaid ("Pre-alignment") and aligned ("Post-alignment") to identify stimulus-responsive neurons that are present across multiple days of imaging.

C) Traces of 3 example neurons during 5 Hz whisker stimulation, tracked across all four 2PCI sessions.

D) Percentage of L2/3 neurons responsive to 5 Hz whisker stimulation across days (n=8 mice). Kruskal-Wallis test.

E) Fraction of cells in each sensory adaptation profile category across days.

F) Mean slope of neurons with a significant linear regression of the AI across days. Mann-Whitney test.

G) Sankey flow diagrams of neurons tracked across two imaging days show dynamic response profiles of neurons from Day 1 to Day 2 and Day 1 to Day 8/9. NR = nonresponsive, NS = nonsignificant, A = adapting, F = facilitating.

H) Percent of longitudinally tracked neurons exhibiting different types of response profiles across imaging sessions. Black brackets: Mann-Whitney test. Green and blue brackets: Friedman test with post-hoc Dunn's test.

Figure 6. Sensory adaptation response dynamics to repetitive whisker stimulation across days in L4 resemble those in L2/3.

A) Example 2PCI FOV in L4 across days in Scnn1a-Cre; Ai162 mouse (scale bar: 100 μm). Top, example FOV on Day 1. Bottom, higher magnification view of a portion of the FOV (red box) across days.

B) Traces of 3 example neurons during 5 Hz whisker stimulation, tracked across all four imaging sessions.

C) Percentage of L4 neurons responsive to 5 Hz whisker stimulation across days (n=5 mice). Kruskal-Wallis test.

D) Fraction of cells in each response profile category.

E) Mean slope of neurons with a significant linear regression of the adaptation index across days. Mann-Whitney test.

F) Sankey flow diagrams showing the adaptation response profiles of L4 neurons across sessions NR = nonresponsive, NS = nonsignificant, A = adapting, F = facilitating.

G) Percent of longitudinally tracked neurons exhibiting certain types of response profile changes between D1 and D2 or D1 and D8 (n=5 mice). Black brackets: Wilcoxon test. Green and blue brackets: Friedman test with post-hoc Dunn's test.

STAR METHODS

RESOURCE AVAILABILITY

Lead contact

Further information and requests for resources and reagents should be directed to and will be fulfilled by the lead contact, Carlos Portera-Cailliau (cpcailliau@mednet.ucla.edu).

Materials availability

This study did not generate new unique reagents.

Data and code availability

All data reported in this paper will be shared by the lead contact upon request. The original code has been deposited at github.com/porteralab as listed in the key resources table. Any additional information required to reanalyze the data reported in this paper is available from the lead contact upon request.

EXPERIMENTAL MODEL AND STUDY PARTICIPANT DETAILS

Experimental animals

All experiments followed the U.S. National Institutes of Health guidelines for animal research, under an animal use protocol (ARC #2007-035) approved by the Chancellor's Animal Research Committee at the University of California, Los Angeles. Experiments used male and female C57BL/6J mice. We crossed Slc17a7-Cre mice (JAX strain # 023527), or the Scnn1a-Cre mice

(JAX strain # 009613) to the Ai162 (GCaMP6s) reporter line (JAX strain # 031562) resulting in Cre-dependent expression of GCaMP6s in Vglut1-positive excitatory neurons, or L4 spiny stellate neurons, respectively. All mice were housed in a vivarium with a reverse 12/12 h light/dark cycle and experiments were performed during the dark cycle. Animals were weaned from their dam at postnatal (P) day 21-22 and then group housed with up to five mice per cage.

METHOD DETAILS

Cranial window surgery

Cranial window surgery was performed on mice at P45-P90, as described previously [64,65]. Mice were anesthetized with isoflurane (5% induction, 1.5-2% maintenance via a nose cone) and placed in a stereotaxic frame (Kopf). Carprofen (5 mg/kg, i.p., Zoetis) and dexamethasone (0.2 mg/kg, i.p., Vet One) were provided for pain relief and mitigation of edema, respectively, on the day of surgery and daily for the next 48 h. A 4 mm diameter craniotomy was performed over the right S1BF and covered with a 4 mm glass coverslip. A custom horseshoe-shaped titanium head bar (3.15 mm wide x 10 mm long) was affixed to the skull with dental cement to secure the animal to the microscope stage. Animals recovered from the procedure and were fully ambulatory within 1 h after the surgery. Carprofen (5 mg/kg, s.c., once daily) was used for analgesia for 3 d post-op.

Thalamus viral injections

For the thalamic virus injections, we performed a 5mm craniotomy over the right S1BF and. ~160 nL of AAV1.Hsyn.GCaMP6s.WPRE.SV40 (Addgene #100843-AAV1; diluted to a working titer of 2E13) was injected at two sites to target the VPM using a Robot Stereotaxic instrument

(Neurostar) coupled to a Kopf stereotaxic frame, and coordinates chosen using the reference atlas on Neurostar (site 1: -1.58 AP, -1.37 ML, 3.61 DV; site 2: -1.7 AP, -1.66 ML and 3.28 DV). At each site a single pulse of ~72 nL was injected using Bregma injector V2. The needle was left in place for 10 min to allow for diffusion and prevent backflow into the needle path. A custom head bar was affixed to the skull and animals allowed to recover. To confirm targeting of VPM, mice were perfused, and injection sites verified by fluorescence microscopy (Zeiss ApoTome2, Zen2 software; 5X objective, 0.3 NA).

Intrinsic signal imaging

Approximately 1 week after cranial window surgery (and at least 3 d before beginning calcium imaging), intrinsic signal imaging was used to map the location of the C2 barrel within barrel cortex, as described previously [66]. The contralateral C2 whisker was gently attached with bone wax to a glass capillary that was coupled to a piezoactuator (Physik Instrumente). Each stimulation trial consisted of a 100 Hz sawtooth stimulation lasting 1.5 s. Thirty stimulation trials were run, with 20 s interstimulus intervals (i.s.i.). The response signal during the whisker stimulations divided by the averaged baseline signal, summed for all trials, was used to generate the C2 barrel map.

2-photon calcium imaging and whisker stimulation

2PCI was performed in awake mice. We used a commercial 2-photon microscope (DIY Bergamo, ThorLabs) equipped with galvo-resonant scanning mirrors, amplified non-cooled GaAsP photomultiplier tubes (Hamamatsu), a 25X objective (1.05 NA, Olympus), and ThorImage software. The microscope was coupled to a Chameleon Ultra II Ti:sapphire laser (Coherent) tuned to 930 nm, and the average power at the sample was kept <150 mW.

We recorded both spontaneous activity and whisker-evoked activity in S1BF. Mice were first habituated to the microscope setup prior to 2PCI. This process lasted ~10 d and involved a gradual progression from basic daily handling (5 min/d) until mice were comfortable with head fixation and body restraint in a plexiglass tube for periods up to 30 min. Mice were considered ready for imaging when they could remain still during sham whisker stimulation, in which the whisker stimulator is placed in front of the mouse but out of reach of its whiskers. The whisker stimulator consisted of a "comb" of von Frey Nylon filaments intercalated between whiskers. This comb was coupled to a piezoactuator (controled by MATLAB), which delivered repetitive deflections of the whiskers in the antero-posterior direction at pre-specified frequencies, durations, and intervals (see below). Calcium imaging was performed at a framerate of 15.1 Hz. For L2/3 recordings in Slc17a7-Cre;Ai162 mice, we recorded responses of ~150-200 neuronal somata at 200-280 μm depth above the C2 barrel within a single field of view (FOV) per animal (measuring 512 x 512 pixels, 533.7 x 533.7 μm). For L4 recordings in Scnn1a-Cre;Ai162 mice, we recorded responses of ~300 neuronal somata at 350-400 μm depth within the C2 barrel (FOV size was the same as in L2/3 recordings).

In a first cohort of Slc17a7-Cre;Ai162 mice (n=8), we first recorded 3 min of spontaneous activity, and then we delivered 2 different whisker stimulation paradigms, in separate movies (with 4-5 min breaks in between each movie), as follows:

- 20 x 5 Hz: stimulus duration 1 s, i.s.i. 3 s
- 20 x 12.5 Hz: stimulus duration 1 s, i.s.i. 3 s

We chose 5 Hz and 12.5 Hz frequencies because they fall within the range of frequencies at which rodents whisk when exploring their surroundings [33], but over the 1 s-long stimulation period,

the latter produced 2.5x more whisker deflections. A 20 s baseline period was included in each whisker stimulation movie before initiating whisker deflections. Mice were given 4–5 min breaks between each stimulation paradigm.

This first cohort of Slc17a7-Cre;Ai162 mice (n=8) was also imaged over several days. The FOV was first identified during the first awake imaging day (Day 1), and then subsequently imaged at +1 d (Day 2), +4 d (Day 5), and +7-8 d (Day 8-9) after the first awake imaging session.

In a second cohort of Slc17a7-Cre;Ai162 mice (n=5), we performed frequency switch experiments (**Figure 3**), first recording 3 min of spontaneous activity followed by the following whisker stimulation paradigms in separate movies:

- 20 x 5 Hz: stimulus duration 1 s, i.s.i. 3 s (Control)
- 20 x 12.5 Hz: stimulus duration 1 s, i.s.i. 3 s (Control)
- 10 x 5 Hz → 10 x 12.5 Hz (Frequency switch)
- 10 x 12.5 Hz → 10 x 5 Hz (Frequency switch)

A third cohort of Slc17a7-Cre;Ai162 mice (n=7) underwent 6 rounds of the 20 x 5 Hz stimulation protocol in a single imaging session, with 4-5 min breaks between rounds. 3 of the mice from this cohort were from the first cohort. As in previous cohorts, 3 min of spontaneous activity was recorded before beginning the first round of whisker stimulation.

A fourth cohort of Slc17a7-Cre;Ai162 mice (n=5) underwent multi-whisker stimulation at different frequencies: 5 Hz, 25 Hz, and 50 Hz. After that, we trimmed all the whiskers on one side of the snout except for one, the C2 whisker. We then repeated the stimulation protocol but with the comb of filaments touching only the C2 whisker. We also used a camera (FLIR BFS-U3-23S3M-C: Monocamera) at 90 fps to record the face in these mice and then FaceMap 0.2.0 [40] to track the relative size of the pupil across the different bouts of whisker stimulation. We used a *Pupil ROI* and applied *corneal correction* within FaceMap. Saturation was adjusted for each

movie, until the pupil tracker tracked the pupil consistently across time. Movies were processed individually to minimize errors due to changes in lighting or positioning. We ensured that lighting or positioning of the camera angle was consistent across experiments. ROI dimensions was exported to and analyzed in MATLAB. Pupil area (pupil.area_smooth) was tracked for each movie and averaged across mice. For tracking whisker deflections, a motSVD ROI was placed over the stimulator and each bout of deflection was recorded. Pupil area was normalized across mice (z-score normalization) and dilation and contraction was calculated by averaging pupil area for each mouse per frequency.

In a fifth cohort of Scnn1a-Cre;Ai162 mice (n=5), we performed the same longitudinal imaging over 8 days but in L4.

Finally, in a sixth cohort of mice (n=5) at 2-3 months of age, we recorded calcium signals from thalamocortical axon boutons. We injected rAAV1-hSyn-GCaMP6s in the VPM nucleus of the thalamus at the time of the cranial window surgery using stereotaxic coordinates (-1.58 AP, -1.37 ML, 3.61 DV and -1.7 AP, -1.66 ML and 3.28 DV). Approximately 1 week after cranial window surgery (and at least a week before beginning calcium imaging), intrinsic imaging was carried out as described earlier. Calcium imaging was performed on a custom-built two-photon microscope with a Chameleon Ultra II Ti:sapphire laser (Coherent), a 20X objective (0.95 numerical aperture, Olympus), and ScanImage software [67]. Whole-field images were acquired at 7.8 Hz (1024 X 128 pixels down sampled to 256 X 128 pixels) [16]. Mice were lightly sedated with chlorprothixene (2 mg/kg, i.p.) and isoflurane (0 – 0.5%) and kept at 37°C using a temperature control device and heating blanket (Harvard Apparatus). Isoflurane was manually adjusted to maintain a breathing rate ranging from 120 –150 breaths/min. Both spontaneous activity and whisker-evoked barrel cortex activity were recorded. Whisker stimulation was delivered by bundling the contralateral whiskers (typically all macrovibrissae of at least 1 cm in length), via soft bone wax, to a glass needle coupled to a piezoactuator. Stimulation was delivered at 5 Hz with the 20X 5 Hz Control stimulation.

To confirm that most whiskers on one side of the snout were being deflected consistently across different sessions (days) during longitudinal imaging, we used a camera (FLIR BFS-U3-23S3M-C: Monocamera) at 30 fps to record the position of the comb of Nylon filaments relative to the whiskers. We cropped the videos, adjusted brightness and contrast, and inverted the color for each movie individually on Shotcut video editor (https://shotcut.org/). Videos were then trained on individual networks on DeepLabCut [42] (resnet 50, shuffle1, iterations 30000). To train the network, three markers were placed on the whisker of interest, one at the base of the whisker, one marker at the point of contact between whisker and filament and the last one at the middle of the shaft. A single marker was also placed on the piezo actuator to track the stimulator movement. After training, the positioning of the markers was exported and analyzed on Python 3. Markers with a likelihood value less than 90 were excluded and the nearest point with a likelihood greater than 90 was substituted instead. Distance of deflections per marker was calculated for each video frame and values were Z-score normalized. Deflections of marker 3, tracking the middle of the whisker, were used for all subsequent analysis in Python.

Neuropixels recordings

Adult mice (P60-90) were anesthetized with isoflurane (5% induction, 1.5-2% maintenance via a nose cone) and placed in a stereotaxic frame. Following skin sterilization with three alternating swabs of 70% ethanol and betadine, an incision was made on the scalp and a titanium horseshoe-shaped headbar was glued to the skull with Metabond adhesive cement. Next, a 2 mm diameter craniotomy was drilled above the cerebellum, just in front of the headbar, and a ground screw was inserted and secured with Metabond. A 1 mm diameter craniotomy was drilled over S1BF (coordinates for now: -1.46 AP, 2.9 ML), through which the shank of a Neuropixels probe (Imec) was carefully inserted at a speed of 10 μm/s using a motorized stereotax (Neurostar).

Dental cement was used to secure the probe base to the skull and a protective 3D-printed case was used to encase the probe. Carprofen (5 mg/kg, s.c.) was administered every 24 h for 3 d.

Electrophysiology recordings were performed using a National Instruments PXIe acquisition system and SpikeGLX software [30,68]. Probe connectors were attached to a headstage and cable connected to the PXIe system while the mouse was being habituated to the rig. For Neuropixels recordings, head-fixed mice were allowed to run on a polystyrene ball treadmill. During behavioral habituation, we recorded daily for 10 min to evaluate the stability of spikes (to ensure that firing rates and amplitude were stable across days). Mice showing a loss of >30% units were excluded from further electrophysiological recordings and analysis.

Analysis

Motion correction and segmentation of 2PCI data: Using a custom MATLAB pipeline already established in the lab (EZcalcium;[69]), calcium movies were motion corrected and semi-automatically segmented. Rigid motion correction was performed in EZcalcium using the following parameters: upsampling factor = 50; max shift = 50 pixels; initial batch size = 200 frames; bin width = 200 frames. Next, we segmented the calcium movies, using EZcalcium for L2/3 data and Suite2P for L4 data.

For EZcalcium, we used the following parameters: Initialization = greedy; Search method = ellipse; Deconvolution = constrained FOOPSI CVX; Autoregression = decay; Estimated regions of interest (ROI) = 140; Estimated ROI width = 15 pixels; Merge threshold = 0.95; Fudge factor = 0.98; Spatial downsampling = 2; Temporal downsampling = 10; Temporal iterations = 3. Following this initial detection of regions of interest (ROIs) we used an initial manual refinement step (also in EZcalcium) to include ROIs that had been missed by the automated segmentation process (typically ~20-30% of final ROIs were added by this manual step). We then proceeded to a ROI refinement step, in which we manually excluded ROIs that had been automatically detected but

were considered to have either spatial contours that were atypical of neurons or because their calcium traces did not show dynamics typical of neurons.

We segmented L4 movies in Suite2P using default settings. Automated ROI exclusion was performed using a custom classifier built using previous L4 data, followed by a manual refinement step to include or exclude ROIs that had been missed by the classifier.

Spike sorting of Neuropixels data: Action potential spikes were sorted with Kilosort2.5 (see Key Resources Table) using default parameters and then manually curated with Phy2 (see Key Resources Table). Post-processing with the following quality metrics was used to isolate single units: interspike interval violation <10%, amplitude cutoff and median amplitude >50 μV [70].

Stimulus responsiveness: Following segmentation, changes in raw fluorescence signal intensity ($\Delta F/F$) were quantified for each ROI using a modified Z score ([F(t) – mean(quietest period)]/SD(quietest period)) as previously described [16]. The proportion of ROIs exhibiting calcium transients that were time-locked to epochs of whisker stimulation was quantified using a either visual inspection or a probabilistic bootstrapping method [16] (**Figure S1A-B**.) These ROIs were deemed stimulus responsive. The peak Z score value for each stimulus-responsive neuron during each epoch of stimulation (i.e., a response peak) was then calculated.

For Neuropixels recordings, we used a receiver operating characteristic (ROC) approach to select stimulus-responsive neurons [71]. Firing rates were calculated in 50 ms time bins for each unit, and we calculated the ROC curve for each unit by comparing its firing rate during each whisker stimulation bout (1 sec) to the firing one second before the stimulation during the interstimulus interval. We determined that a neuron was stimulus responsive if the area under the curve (AUC) exceeded 0.5 and was greater than 97.5% in a null distribution of AUCs. The null

distribution of AUCs was generated by shuffling the firing rates and recalculating the AUC over 1,000 permutations.

Response reliability: In our quantification of response reliability (**Figure S2A-B** and **Figure S10B**) a neuron was considered responsive during a stimulation bout if it had a response peak with a Z score > 3.

Adaptation index: To quantify adaptation/facilitation for each neuron, an adaptation index (AI) was computed by regressing the response peak magnitude during stimulations 1-15 against stimulation number (i.e., fitting a line to the response peaks for stimulations 1-15 for each cell). Cells with significant negative regression slopes (i.e. a negative slope with a regression p-value of < 0.1) were classified as adapting, while cells with significant positive regression slopes were classified as facilitating. Cells were classified as nonsignificant if their regression slopes were not significant ($p \geq 0.1$). We chose 15 stimulations because in some mice there was motion artifact around stimulations 18-20. In rare cases of motion artifact before stimulation 15, response peak magnitudes during the motion artifact period were extrapolated by calculating the mean of the two response peaks directly before and after the motion artifact period.

For **Figs. 5** and **6**, adapting and facilitating cells were divided into strong and weak subcategories. Cells with a slope > 1 were classified as strongly facilitating, while cells with a slope less than -1 were classified as strongly adapting. Cells with a significant slope of ≤ 1 or ≥ -1 were classified as weakly facilitating and weakly adapting, respectively.

We also tested an alternative method of quantifying adaptation, similar to what we had used in a previous publication [16]. We calculated the mean response peak magnitude for stimulations 1-5 (Mean, stims 1-5) and for stimulations 10-15 (Mean, stims 11-15), and computed an AI using the following formula: [(Mean, stims 1-5) – (Mean, stims 11-15)] / [(Mean, stims 1-5) + (Mean, stims 11-15)]. Cutoffs of ±0.4 were set based on the distribution of values (**Figure S3B**).

Longitudinal imaging analysis: To identify the same ROIs across days in our longitudinal imaging experiments, we employed CellReg (v1.4.9; [41]), a probabilistic method for tracking neurons longitudinally in calcium movies. We then calculated the proportion of longitudinally tracked ROIs that maintained or changed their response profile (adapting, facilitating, intermediate, non-responsive) between pairs of imaging sessions (e.g., Day 1 vs. Day 2, Day 1 vs. Day 5, Day 1 vs. Day 8/9). We also assessed the number of ROIs that became non-responsive on the second day in the pair of imaging sessions. For Suppl. Fig 6c and Suppl. Figure 7c, we tracked the same ROIs across all imaging days (either 3 or 4) and calculated the percentage of cells that exhibited major or mild changes in response profile.

QUANTIFICATION AND STATISTICAL ANALYSIS

Results were plotted using Prism 9 and MATLAB and tested for statistical significance using Prism 9. Central tendencies are reported in the main text as mean plus or minus standard error of the mean (S.E.M.). Means were either calculated as an average of mice (Figs. 1H, 1J, 3B-D, 4E, 5H, 6G; Figs. S1B-C, S3D, 3G-H, S4B-C, S4E, S5I, S6A, S6C, S7B, S11C-D, S11G-H), or as an average of cells pooled across all mice (Figs. 2F, 3E-H, 4D, 5F, 6E; Figs. S3H, S4E, S6B, S6D, S7C, S8A-C, S10B). Tests for normality were always completed before performing statistical tests. For any exclusion of outlier values, the ROUT method (Q = 1%) was used. All statistical tests are reported in figure legends, and corresponding p-values are reported in figures.

REFERENCES

1. Adibi, M., and Lampl, I. (2021). Sensory Adaptation in the Whisker-Mediated Tactile System: Physiology, Theory, and Function. Front Neurosci *15*, 770011. 10.3389/fnins.2021.770011.
2. Whitmire, C.J., and Stanley, G.B. (2016). Rapid Sensory Adaptation Redux: A Circuit Perspective. Neuron *92*, 298-315. 10.1016/j.neuron.2016.09.046.
3. Barlow, h. (1961). Possible principles underlying the transformations of sensory messages. Sensory communication *13*, 217-234.
4. Maravall, M., Petersen, R.S., Fairhall, A.L., Arabzadeh, E., and Diamond, M.E. (2007). Shifts in coding properties and maintenance of information transmission during adaptation in barrel cortex. PLoS Biol *5*, e19. 10.1371/journal.pbio.0050019.
5. Adibi, M., McDonald, J.S., Clifford, C.W., and Arabzadeh, E. (2013). Adaptation improves neural coding efficiency despite increasing correlations in variability. J Neurosci *33*, 2108-2120. 10.1523/JNEUROSCI.3449-12.2013.
6. Brenner, N., Bialek, W., and de Ruyter van Steveninck, R. (2000). Adaptive rescaling maximizes information transmission. Neuron *26*, 695-702. 10.1016/s0896-6273(00)81205-2.
7. Tannan, V., Whitsel, B.L., and Tommerdahl, M.A. (2006). Vibrotactile adaptation enhances spatial localization. Brain Res *1102*, 109-116. 10.1016/j.brainres.2006.05.037.
8. Ollerenshaw, D.R., Zheng, H.J.V., Millard, D.C., Wang, Q., and Stanley, G.B. (2014). The adaptive trade-off between detection and discrimination in cortical representations and behavior. Neuron *81*, 1152-1164. 10.1016/j.neuron.2014.01.025.
9. Keller, G.B., and Mrsic-Flogel, T.D. (2018). Predictive Processing: A Canonical Cortical Computation. Neuron *100*, 424-435. 10.1016/j.neuron.2018.10.003.
10. Weber, A.I., Krishnamurthy, K., and Fairhall, A.L. (2019). Coding Principles in Adaptation. Annu Rev Vis Sci *5*, 427-449. 10.1146/annurev-vision-091718-014818.
11. Tommerdahl, M., Tannan, V., Cascio, C.J., Baranek, G.T., and Whitsel, B.L. (2007). Vibrotactile adaptation fails to enhance spatial localization in adults with autism. Brain Res *1154*, 116-123. 10.1016/j.brainres.2007.04.032.
12. Puts, N.A., Wodka, E.L., Tommerdahl, M., Mostofsky, S.H., and Edden, R.A. (2014). Impaired tactile processing in children with autism spectrum disorder. J Neurophysiol *111*, 1803-1811. 10.1152/jn.00890.2013.
13. Green, S.A., Hernandez, L., Tottenham, N., Krasileva, K., Bookheimer, S.Y., and Dapretto, M. (2015). Neurobiology of Sensory Overresponsivity in Youth With Autism Spectrum Disorders. JAMA Psychiatry *72*, 778-786. 10.1001/jamapsychiatry.2015.0737.
14. Ethridge, L.E., White, S.P., Mosconi, M.W., Wang, J., Byerly, M.J., and Sweeney, J.A. (2016). Reduced habituation of auditory evoked potentials indicate cortical hyper-excitability in Fragile X Syndrome. Transl Psychiatry *6*, e787. 10.1038/tp.2016.48.
15. Miller, L.J., McIntosh, D.N., McGrath, J., Shyu, V., Lampe, M., Taylor, A.K., Tassone, F., Neitzel, K., Stackhouse, T., and Hagerman, R.J. (1999). Electrodermal responses to sensory stimuli in individuals with fragile X syndrome: a preliminary report. American journal of medical genetics *83*, 268-279.

16. He, C.X., Cantu, D.A., Mantri, S.S., Zeiger, W.A., Goel, A., and Portera-Cailliau, C. (2017). Tactile Defensiveness and Impaired Adaptation of Neuronal Activity in the Fmr1 Knock-Out Mouse Model of Autism. J Neurosci *37*, 6475-6487. 10.1523/JNEUROSCI.0651-17.2017.
17. Kourdougli, N., Suresh, A., Liu, B., Juarez, P., Lin, A., Chung, D.T., Graven Sams, A., Gandal, M.J., Martinez-Cerdeno, V., Buonomano, D.V., et al. (2023). Improvement of sensory deficits in fragile X mice by increasing cortical interneuron activity after the critical period. Neuron *111*, 2863-2880. 10.1016/j.neuron.2023.06.009.
18. Chung, S., Li, X., and Nelson, S.B. (2002). Short-term depression at thalamocortical synapses contributes to rapid adaptation of cortical sensory responses in vivo. Neuron *34*, 437-446. 10.1016/s0896-6273(02)00659-1.
19. Khatri, V., Hartings, J.A., and Simons, D.J. (2004). Adaptation in thalamic barreloid and cortical barrel neurons to periodic whisker deflections varying in frequency and velocity. J Neurophysiol *92*, 3244-3254. 10.1152/jn.00257.2004.
20. Ulanovsky, N., Las, L., and Nelken, I. (2003). Processing of low-probability sounds by cortical neurons. Nat Neurosci *6*, 391-398. 10.1038/nn1032.
21. Wark, B., Fairhall, A., and Rieke, F. (2009). Timescales of inference in visual adaptation. Neuron *61*, 750-761. 10.1016/j.neuron.2009.01.019.
22. Dragoi, V., Sharma, J., and Sur, M. (2000). Adaptation-induced plasticity of orientation tuning in adult visual cortex. Neuron *28*, 287-298. 10.1016/s0896-6273(00)00103-3.
23. Kheradpezhouh, E., Adibi, M., and Arabzadeh, E. (2017). Response dynamics of rat barrel cortex neurons to repeated sensory stimulation. Sci Rep *7*, 11445. 10.1038/s41598-017-11477-6.
24. Castro-Alamancos, M.A. (2004). Absence of rapid sensory adaptation in neocortex during information processing states. Neuron *41*, 455-464. 10.1016/s0896-6273(03)00853-5.
25. Kastner, D.B., and Baccus, S.A. (2011). Coordinated dynamic encoding in the retina using opposing forms of plasticity. Nat Neurosci *14*, 1317-1322. 10.1038/nn.2906.
26. Dhruv, N.T., Tailby, C., Sokol, S.H., and Lennie, P. (2011). Multiple adaptable mechanisms early in the primate visual pathway. J Neurosci *31*, 15016-15025. 10.1523/JNEUROSCI.0890-11.2011.
27. Phillips, E.A.K., Schreiner, C.E., and Hasenstaub, A.R. (2017). Diverse effects of stimulus history in waking mouse auditory cortex. J Neurophysiol *118*, 1376-1393. 10.1152/jn.00094.2017.
28. Rule, M.E., O'Leary, T., and Harvey, C.D. (2019). Causes and consequences of representational drift. Curr Opin Neurobiol *58*, 141-147. 10.1016/j.conb.2019.08.005.
29. Grienberger, C., Giovannucci, A., Zeiger, W., and Portera-Cailliau, C. (2022). Two-photon calcium imaging of neuronal activity. Nat Rev Methods Primers *2*. 10.1038/s43586-022-00147-1.
30. Jun, J.J., Steinmetz, N.A., Siegle, J.H., Denman, D.J., Bauza, M., Barbarits, B., Lee, A.K., Anastassiou, C.A., Andrei, A., Aydin, C., et al. (2017). Fully integrated silicon probes for high-density recording of neural activity. Nature *551*, 232-236. 10.1038/nature24636.
31. Harris, J.A., Hirokawa, K.E., Sorensen, S.A., Gu, H., Mills, M., Ng, L.L., Bohn, P., Mortrud, M., Ouellette, B., Kidney, J., et al. (2014). Anatomical characterization of Cre driver mice

for neural circuit mapping and manipulation. Front Neural Circuits *8*, 76. 10.3389/fncir.2014.00076.

32. Daigle, T.L., Madisen, L., Hage, T.A., Valley, M.T., Knoblich, U., Larsen, R.S., Takeno, M.M., Huang, L., Gu, H., Larsen, R., et al. (2018). A Suite of Transgenic Driver and Reporter Mouse Lines with Enhanced Brain-Cell-Type Targeting and Functionality. Cell *174*, 465-480 e422. 10.1016/j.cell.2018.06.035.
33. Megevand, P., Troncoso, E., Quairiaux, C., Muller, D., Michel, C.M., and Kiss, J.Z. (2009). Long-term plasticity in mouse sensorimotor circuits after rhythmic whisker stimulation. J Neurosci *29*, 5326-5335. 10.1523/JNEUROSCI.5965-08.2009.
34. Clancy, K.B., Schnepel, P., Rao, A.T., and Feldman, D.E. (2015). Structure of a single whisker representation in layer 2 of mouse somatosensory cortex. J Neurosci *35*, 3946-3958. 10.1523/JNEUROSCI.3887-14.2015.
35. Natan, R.G., Briguglio, J.J., Mwilambwe-Tshilobo, L., Jones, S.I., Aizenberg, M., Goldberg, E.M., and Geffen, M.N. (2015). Complementary control of sensory adaptation by two types of cortical interneurons. Elife *4*. 10.7554/eLife.09868.
36. Natan, R.G., Rao, W., and Geffen, M.N. (2017). Cortical Interneurons Differentially Shape Frequency Tuning following Adaptation. Cell Rep *21*, 878-890. 10.1016/j.celrep.2017.10.012.
37. Seay, M.J., Natan, R.G., Geffen, M.N., and Buonomano, D.V. (2020). Differential Short-Term Plasticity of PV and SST Neurons Accounts for Adaptation and Facilitation of Cortical Neurons to Auditory Tones. J Neurosci *40*, 9224-9235. 10.1523/JNEUROSCI.0686-20.2020.
38. Sachdev, R.N., Krause, M.R., and Mazer, J.A. (2012). Surround suppression and sparse coding in visual and barrel cortices. Front Neural Circuits *6*, 43. 10.3389/fncir.2012.00043.
39. Ferezou, I., Haiss, F., Gentet, L.J., Aronoff, R., Weber, B., and Petersen, C.C. (2007). Spatiotemporal dynamics of cortical sensorimotor integration in behaving mice. Neuron *56*, 907-923. 10.1016/j.neuron.2007.10.007.
40. Syeda, A., Zhong, L., Tung, R., Long, W., Pachitariu, M., and Stringer, C. (2024). Facemap: a framework for modeling neural activity based on orofacial tracking. Nat Neurosci *27*, 187-195. 10.1038/s41593-023-01490-6.
41. Sheintuch, L., Rubin, A., Brande-Eilat, N., Geva, N., Sadeh, N., Pinchasof, O., and Ziv, Y. (2017). Tracking the Same Neurons across Multiple Days in Ca(2+) Imaging Data. Cell Rep *21*, 1102-1115. 10.1016/j.celrep.2017.10.013.
42. Mathis, A., Mamidanna, P., Cury, K.M., Abe, T., Murthy, V.N., Mathis, M.W., and Bethge, M. (2018). DeepLabCut: markerless pose estimation of user-defined body parts with deep learning. Nat Neurosci *21*, 1281-1289. 10.1038/s41593-018-0209-y.
43. Petersen, C.C. (2007). The functional organization of the barrel cortex. Neuron *56*, 339-355. S0896-6273(07)00715-5 [pii] 10.1016/j.neuron.2007.09.017.
44. Jones, E.G., and Wise, S.P. (1977). Size, laminar and columnar distribution of efferent cells in the sensory-motor cortex of monkeys. J Comp Neurol *175*, 391-438. 10.1002/cne.901750403.
45. Naskar, S., Qi, J., Pereira, F., Gerfen, C.R., and Lee, S. (2021). Cell-type-specific recruitment of GABAergic interneurons in the primary somatosensory cortex by long-range inputs. Cell Rep *34*, 108774. 10.1016/j.celrep.2021.108774.

46. Voelcker, B., Pancholi, R., and Peron, S. (2022). Transformation of primary sensory cortical representations from layer 4 to layer 2. Nat Commun *13*, 5484. 10.1038/s41467-022-33249-1.
47. Musall, S., Haiss, F., Weber, B., and von der Behrens, W. (2017). Deviant Processing in the Primary Somatosensory Cortex. Cereb Cortex *27*, 863-876. 10.1093/cercor/bhv283.
48. Derdikman, D., Yu, C., Haidarliu, S., Bagdasarian, K., Arieli, A., and Ahissar, E. (2006). Layer-specific touch-dependent facilitation and depression in the somatosensory cortex during active whisking. J Neurosci *26*, 9538-9547. 10.1523/JNEUROSCI.0918-06.2006.
49. Brecht, M., and Sakmann, B. (2002). Dynamic representation of whisker deflection by synaptic potentials in spiny stellate and pyramidal cells in the barrels and septa of layer 4 rat somatosensory cortex. J Physiol *543*, 49-70. 10.1113/jphysiol.2002.018465.
50. Ego-Stengel, V., Mello e Souza, T., Jacob, V., and Shulz, D.E. (2005). Spatiotemporal characteristics of neuronal sensory integration in the barrel cortex of the rat. J Neurophysiol *93*, 1450-1467. 10.1152/jn.00912.2004.
51. Crochet, S., and Petersen, C.C. (2006). Correlating whisker behavior with membrane potential in barrel cortex of awake mice. Nature neuroscience *9*, 608-610. 10.1038/nn1690.
52. Hong, Y.K., Lacefield, C.O., Rodgers, C.C., and Bruno, R.M. (2018). Sensation, movement and learning in the absence of barrel cortex. Nature *561*, 542-546. 10.1038/s41586-018-0527-y.
53. Collins Rodriguez, A., Loft, M.S.E., Schiessl, I., Maravall, M., and Pertersen, R. (2022). Sensory adaptation in the barrel cortex during active sensation in the awake, behaving mouse. BioRxiv. https://doi.org/10.1101/2022.07.07.499259.
54. Garabedian, C.E., Jones, S.R., Merzenich, M.M., Dale, A., and Moore, C.I. (2003). Band-pass response properties of rat SI neurons. J Neurophysiol *90*, 1379-1391. 10.1152/jn.01158.2002.
55. Hamm, J.P., and Yuste, R. (2016). Somatostatin Interneurons Control a Key Component of Mismatch Negativity in Mouse Visual Cortex. Cell Rep *16*, 597-604. 10.1016/j.celrep.2016.06.037.
56. Wang, H.C., LeMessurier, A.M., and Feldman, D.E. (2022). Tuning instability of non-columnar neurons in the salt-and-pepper whisker map in somatosensory cortex. Nat Commun *13*, 6611. 10.1038/s41467-022-34261-1.
57. Castro-Alamancos, M.A., and Oldford, E. (2002). Cortical sensory suppression during arousal is due to the activity-dependent depression of thalamocortical synapses. J Physiol *541*, 319-331. 10.1113/jphysiol.2002.016857.
58. Wright, N.C., Borden, P.Y., Liew, Y.J., Bolus, M.F., Stoy, W.M., Forest, C.R., and Stanley, G.B. (2021). Rapid Cortical Adaptation and the Role of Thalamic Synchrony during Wakefulness. J Neurosci *41*, 5421-5439. 10.1523/JNEUROSCI.3018-20.2021.
59. Heiss, J.E., Katz, Y., Ganmor, E., and Lampl, I. (2008). Shift in the balance between excitation and inhibition during sensory adaptation of S1 neurons. The Journal of neuroscience : the official journal of the Society for Neuroscience *28*, 13320-13330. 10.1523/JNEUROSCI.2646-08.2008.

60. Rao, R.P., and Ballard, D.H. (1999). Predictive coding in the visual cortex: a functional interpretation of some extra-classical receptive-field effects. Nat Neurosci *2*, 79-87. 10.1038/4580.
61. Aronoff, R., Matyas, F., Mateo, C., Ciron, C., Schneider, B., and Petersen, C.C. (2010). Long-range connectivity of mouse primary somatosensory barrel cortex. Eur J Neurosci *31*, 2221-2233. 10.1111/j.1460-9568.2010.07264.x.
62. Petreanu, L., Mao, T., Sternson, S.M., and Svoboda, K. (2009). The subcellular organization of neocortical excitatory connections. Nature *457*, 1142-1145. 10.1038/nature07709.
63. Mao, T., Kusefoglu, D., Hooks, B.M., Huber, D., Petreanu, L., and Svoboda, K. (2011). Long-range neuronal circuits underlying the interaction between sensory and motor cortex. Neuron *72*, 111-123. 10.1016/j.neuron.2011.07.029.
64. Mostany, R., and Portera-Cailliau, C. (2008). A craniotomy surgery procedure for chronic brain imaging. J Vis Exp. 680 [pii]
10.3791/680.
65. Holtmaat, A., Bonhoeffer, T., Chow, D.K., Chuckowree, J., De Paola, V., Hofer, S.B., Hubener, M., Keck, T., Knott, G., Lee, W.C., et al. (2009). Long-term, high-resolution imaging in the mouse neocortex through a chronic cranial window. Nat Protoc *4*, 1128-1144. nprot.2009.89 [pii]
10.1038/nprot.2009.89.
66. Zeiger, W.A., Marosi, M., Saggi, S., Noble, N., Samad, I., and Portera-Cailliau, C. (2021). Barrel cortex plasticity after photothrombotic stroke involves potentiating responses of pre-existing circuits but not functional remapping to new circuits. Nat Commun *12*, 3972. 10.1038/s41467-021-24211-8.
67. Pologruto, T.A., Sabatini, B.L., and Svoboda, K. (2003). ScanImage: flexible software for operating laser scanning microscopes. Biomed Eng Online *2*, 13. 10.1186/1475-925X-2-13.
68. Juavinett, A.L., Bekheet, G., and Churchland, A.K. (2019). Chronically implanted Neuropixels probes enable high-yield recordings in freely moving mice. Elife *8*. 10.7554/eLife.47188.
69. Cantu, D.A., Wang, B., Gongwer, M.W., He, C.X., Goel, A., Suresh, A., Kourdougli, N., Arroyo, E.D., Zeiger, W., and Portera-Cailliau, C. (2020). EZcalcium: Open-Source Toolbox for Analysis of Calcium Imaging Data. Front Neural Circuits *14*, 25. 10.3389/fncir.2020.00025.
70. Hill, D.N., Mehta, S.B., and Kleinfeld, D. (2011). Quality metrics to accompany spike sorting of extracellular signals. J Neurosci *31*, 8699-8705. 10.1523/JNEUROSCI.0971-11.2011.
71. Mazuski, C., and O'Keefe, J. (2022). Representation of ethological events by basolateral amygdala neurons. Cell Rep *39*, 110921. 10.1016/j.celrep.2022.110921.

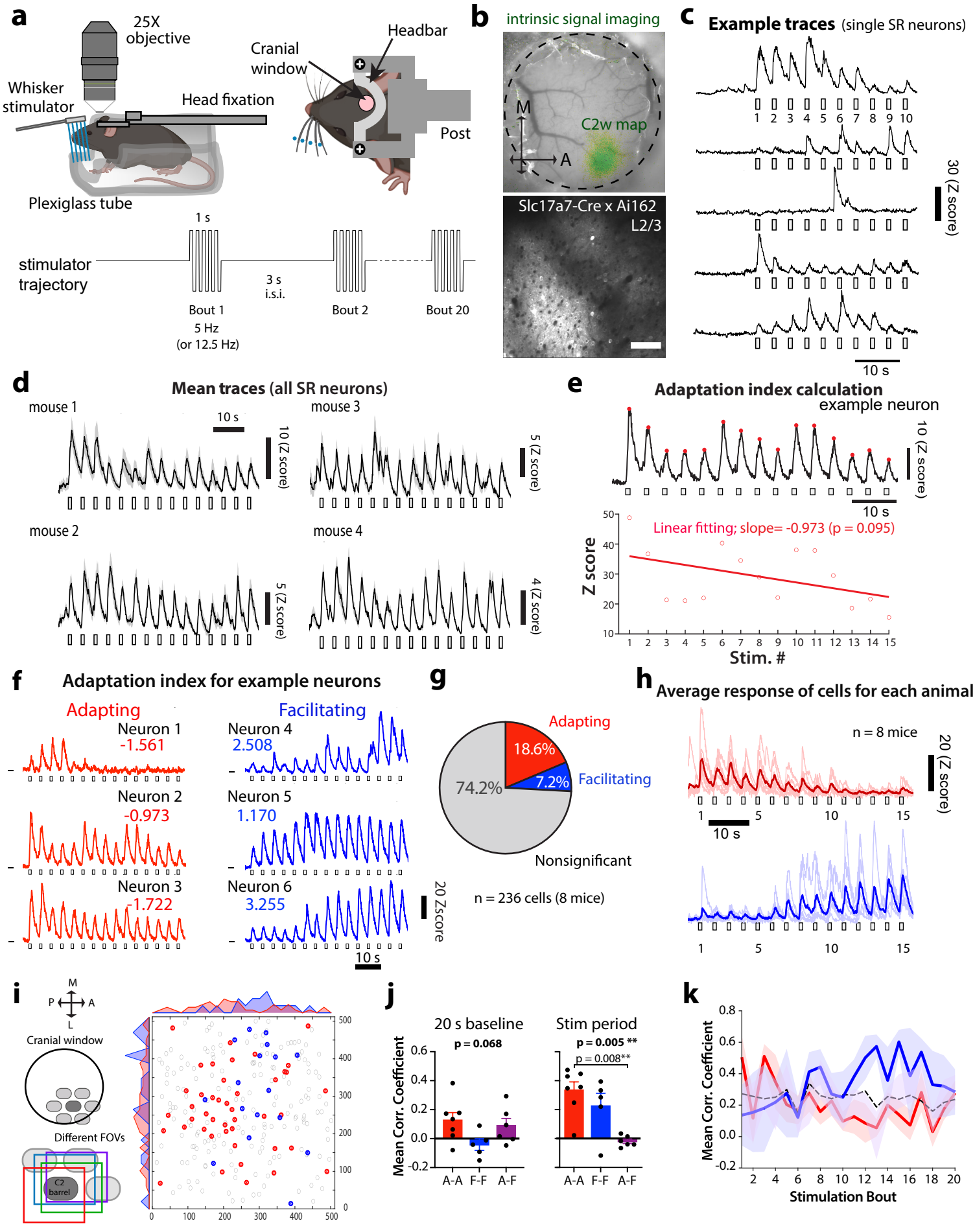
a
25X objective
Whisker stimulator
Head fixation
Cranial window
Headbar
Post
Plexiglass tube
1 s
stimulator trajectory
3 s i.s.i.
Bout 1
5 Hz
(or 12.5 Hz)
Bout 2
Bout 20
b
intrinsic signal imaging
M
A
C2w map
Slc17a7-Cre x Ai162
L2/3
c
Example traces (single SR neurons)
1 2 3 4 5 6 7 8 9 10
30 (Z score)
10 s
d
Mean traces (all SR neurons)
mouse 1
10 s
10 (Z score)
mouse 3
5 (Z score)
mouse 2
5 (Z score)
mouse 4
4 (Z score)
e
Adaptation index calculation
example neuron
10 (Z score)
10 s
Linear fitting; slope= -0.973 (p = 0.095)
Z score
Stim. #
f
Adaptation index for example neurons
Adapting
Neuron 1
-1.561
Neuron 2
-0.973
Neuron 3
-1.722
Facilitating
Neuron 4
2.508
Neuron 5
1.170
Neuron 6
3.255
20 Zscore
10 s
g
Adapting
18.6%
7.2%
Facilitating
74.2%
Nonsignificant
n = 236 cells (8 mice)
h
Average response of cells for each animal
n = 8 mice
20 (Z score)
10 s
i
M
P
A
L
Cranial window
Different FOVs
C2 barrel
j
20 s baseline
p = 0.068
Stim period
p = 0.005 **
p = 0.008**
Mean Corr. Coefficient
A-A F-F A-F
k
Mean Corr. Coefficient
Stimulation Bout

FIGURE 1

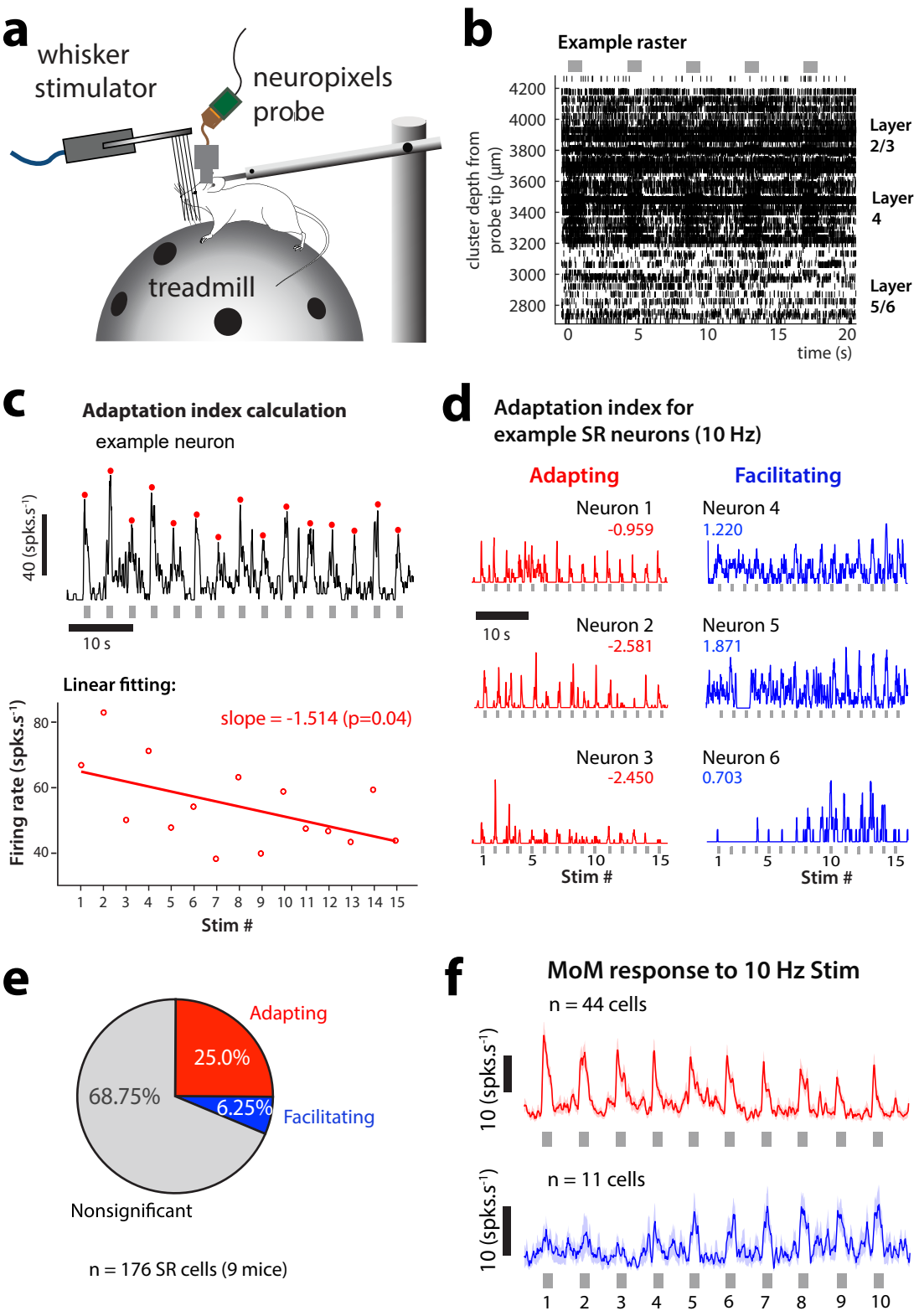
a
whisker stimulator
neuropixels probe
treadmill
b
Example raster
cluster depth from probe tip (µm)
4200
4000
3800
3600
3400
3200
3000
2800
0
5
10
15
20
time (s)
Layer 2/3
Layer 4
Layer 5/6
c
Adaptation index calculation
example neuron
40 (spks.s-1)
10 s
Linear fitting:
slope = -1.514 (p=0.04)
Firing rate (spks.s-1)
80
60
40
1 2 3 4 5 6 7 8 9 10 11 12 13 14 15
Stim #
d
Adaptation index for example SR neurons (10 Hz)
Adapting
Facilitating
Neuron 1
-0.959
Neuron 4
1.220
10 s
Neuron 2
-2.581
Neuron 5
1.871
Neuron 3
-2.450
Neuron 6
0.703
1 5 10 15
Stim #
e
Adapting
25.0%
68.75%
6.25%
Facilitating
Nonsignificant
n = 176 SR cells (9 mice)
f
MoM response to 10 Hz Stim
n = 44 cells
10 (spks.s-1)
n = 11 cells
10 (spks.s-1)
1 2 3 4 5 6 7 8 9 10

FIGURE 2

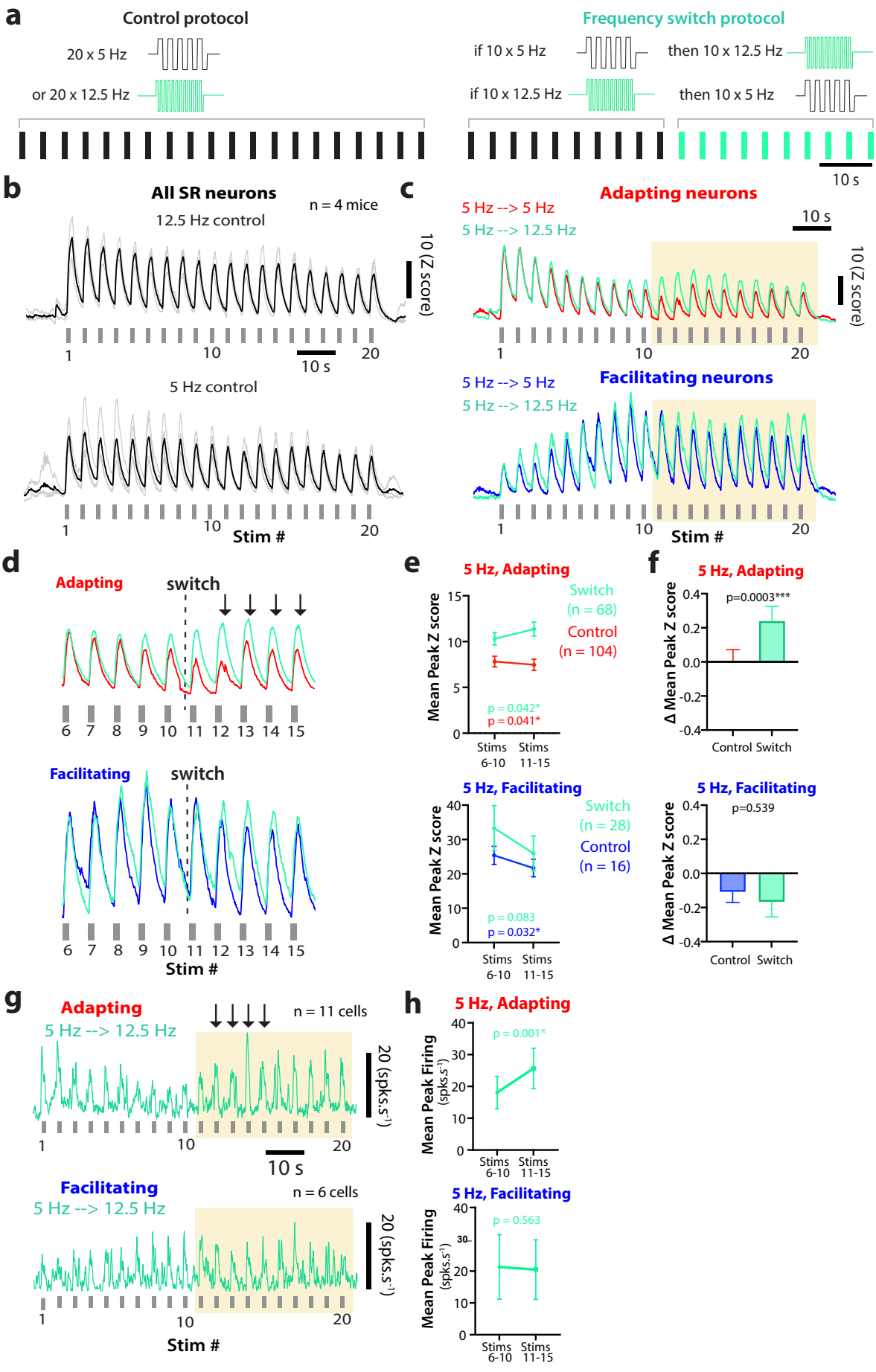
a
Control protocol
20 x 5 Hz
or 20 x 12.5 Hz
Frequency switch protocol
if 10 x 5 Hz
then 10 x 12.5 Hz
if 10 x 12.5 Hz
then 10 x 5 Hz
10 s
b
All SR neurons
n = 4 mice
12.5 Hz control
10 (Z score)
10 s
5 Hz control
Stim #
c
Adapting neurons
5 Hz --> 5 Hz
5 Hz --> 12.5 Hz
10 s
10 (Z score)
Facilitating neurons
d
Adapting
switch
Facilitating
Stim #
e
5 Hz, Adapting
Switch (n = 68)
Control (n = 104)
Mean Peak Z score
p = 0.042*
p = 0.041*
Stims 6-10
Stims 11-15
5 Hz, Facilitating
Switch (n = 28)
Control (n = 16)
p = 0.083
p = 0.032*
f
5 Hz, Adapting
p=0.0003***
Δ Mean Peak Z score
Control Switch
5 Hz, Facilitating
p=0.539
g
Adapting
5 Hz --> 12.5 Hz
n = 11 cells
20 (spks.s-1)
10 s
Facilitating
n = 6 cells
Stim #
h
5 Hz, Adapting
p = 0.001*
Mean Peak Firing (spks.s-1)
5 Hz, Facilitating
p = 0.563

FIGURE 3

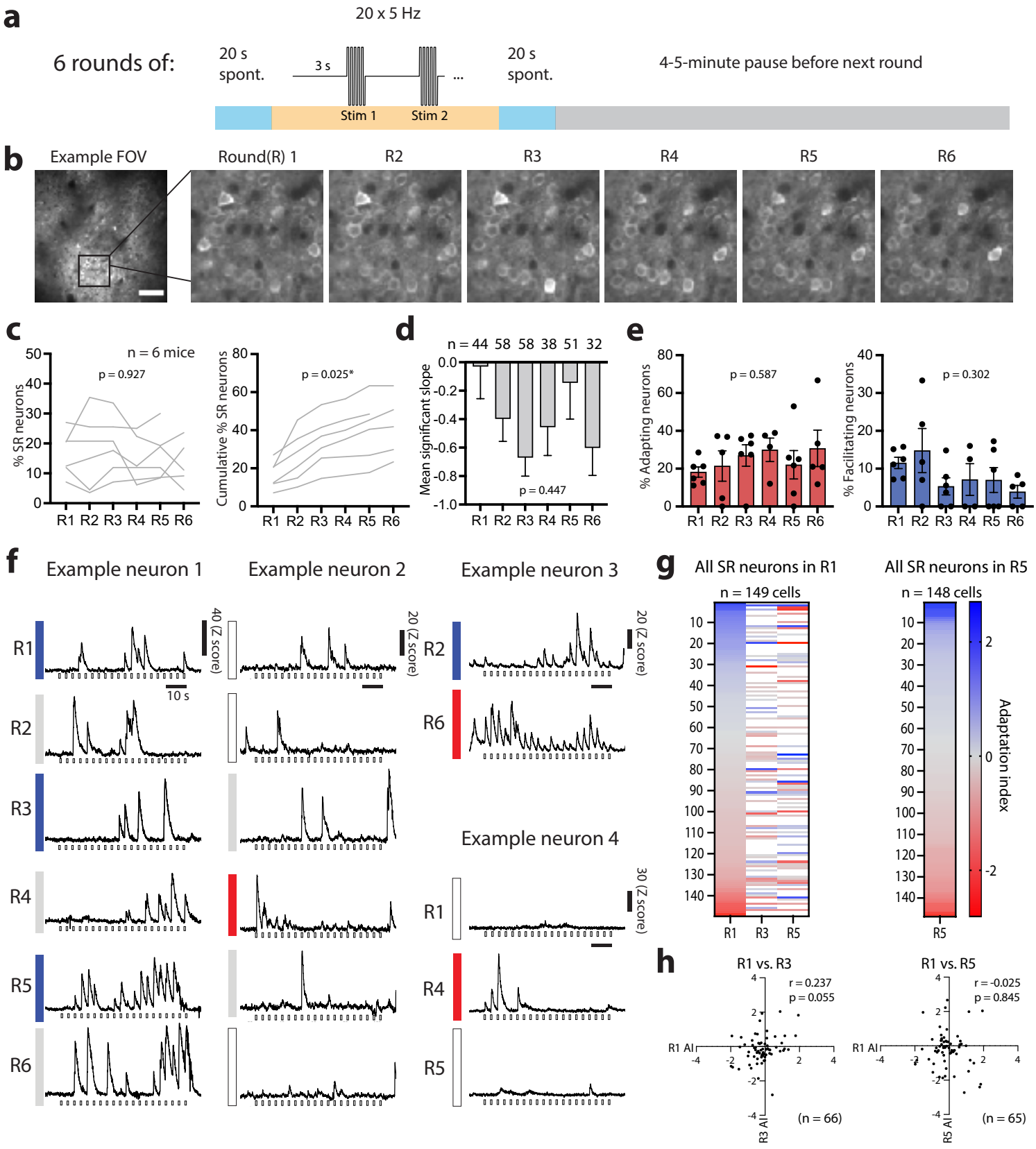
a
20 x 5 Hz
6 rounds of:
20 s spont.
3 s
...
20 s spont.
4-5-minute pause before next round
Stim 1
Stim 2
b
Example FOV
Round(R) 1
R2
R3
R4
R5
R6
c
n = 6 mice
p = 0.927
% SR neurons
p = 0.025*
Cumulative % SR neurons
R1 R2 R3 R4 R5 R6
d
n = 44 58 58 38 51 32
Mean significant slope
p = 0.447
e
% Adapting neurons
p = 0.587
% Facilitating neurons
p = 0.302
f
Example neuron 1
Example neuron 2
Example neuron 3
Example neuron 4
10 s
40 (Z score)
20 (Z score)
30 (Z score)
g
All SR neurons in R1
n = 149 cells
All SR neurons in R5
n = 148 cells
Adaptation index
h
R1 vs. R3
r = 0.237
p = 0.055
R1 AI
R3 AI
(n = 66)
R1 vs. R5
r = -0.025
p = 0.845
R5 AI
(n = 65)

FIGURE 4

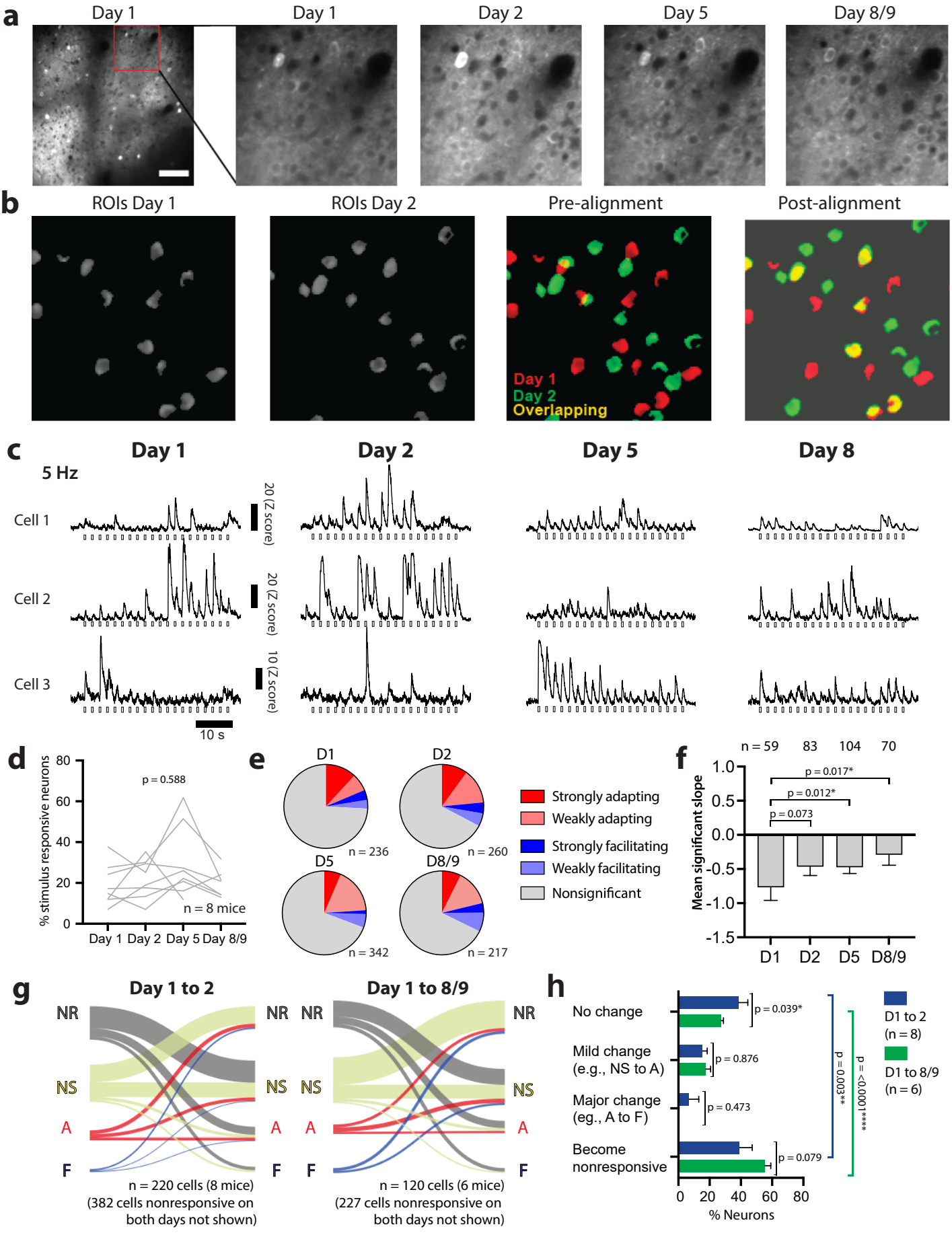
a
Day 1
Day 1
Day 2
Day 5
Day 8/9
b
ROIs Day 1
ROIs Day 2
Pre-alignment
Post-alignment
Day 1
Day 2
Overlapping
c
Day 1
Day 2
Day 5
Day 8
5 Hz
Cell 1
Cell 2
Cell 3
20 (Z score)
20 (Z score)
10 (Z score)
10 s
d
% stimulus responsive neurons
p = 0.588
n = 8 mice
Day 1 Day 2 Day 5 Day 8/9
e
D1
D2
D5
D8/9
n = 236
n = 260
n = 342
n = 217
Strongly adapting
Weakly adapting
Strongly facilitating
Weakly facilitating
Nonsignificant
f
n = 59 83 104 70
p = 0.017*
p = 0.012*
p = 0.073
Mean significant slope
D1 D2 D5 D8/9
g
Day 1 to 2
Day 1 to 8/9
NR
NS
A
F
n = 220 cells (8 mice)
(382 cells nonresponsive on
both days not shown)
n = 120 cells (6 mice)
(227 cells nonresponsive on
both days not shown)
h
No change
Mild change
(e.g., NS to A)
Major change
(eg., A to F)
Become
nonresponsive
p = 0.039*
p = 0.876
p = 0.473
p = 0.079
p = 0.003**
p = <0.0001****
D1 to 2
(n = 8)
D1 to 8/9
(n = 6)
% Neurons

FIGURE 5

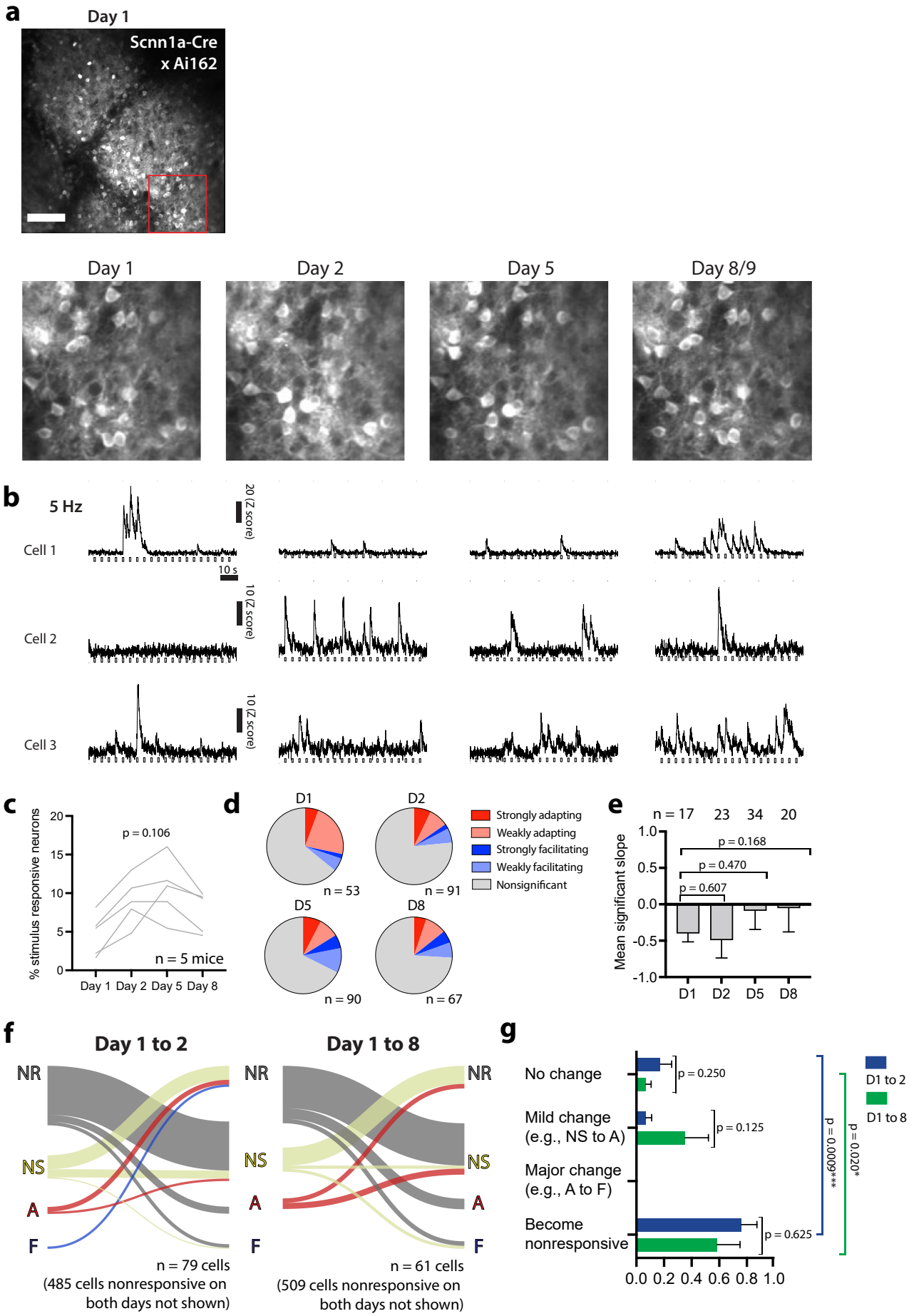
a
Day 1
Scnn1a-Cre
x Ai162
Day 1
Day 2
Day 5
Day 8/9
b
5 Hz
Cell 1
Cell 2
Cell 3
20 (Z score)
10 (Z score)
10 (Z score)
10 s
c
% stimulus responsive neurons
p = 0.106
n = 5 mice
Day 1 Day 2 Day 5 Day 8
d
D1
D2
D5
D8
n = 53
n = 91
n = 90
n = 67
Strongly adapting
Weakly adapting
Strongly facilitating
Weakly facilitating
Nonsignificant
e
n = 17 23 34 20
Mean significant slope
p = 0.168
p = 0.470
p = 0.607
D1 D2 D5 D8
f
Day 1 to 2
Day 1 to 8
NR
NS
A
F
n = 79 cells
(485 cells nonresponsive on
both days not shown)
n = 61 cells
(509 cells nonresponsive on
both days not shown)
g
No change
Mild change
(e.g., NS to A)
Major change
(e.g., A to F)
Become
nonresponsive
p = 0.250
p = 0.125
p = 0.625
p = 0.0009***
p = 0.020*
D1 to 2
D1 to 8
0.0 0.2 0.4 0.6 0.8 1.0

FIGURE 6

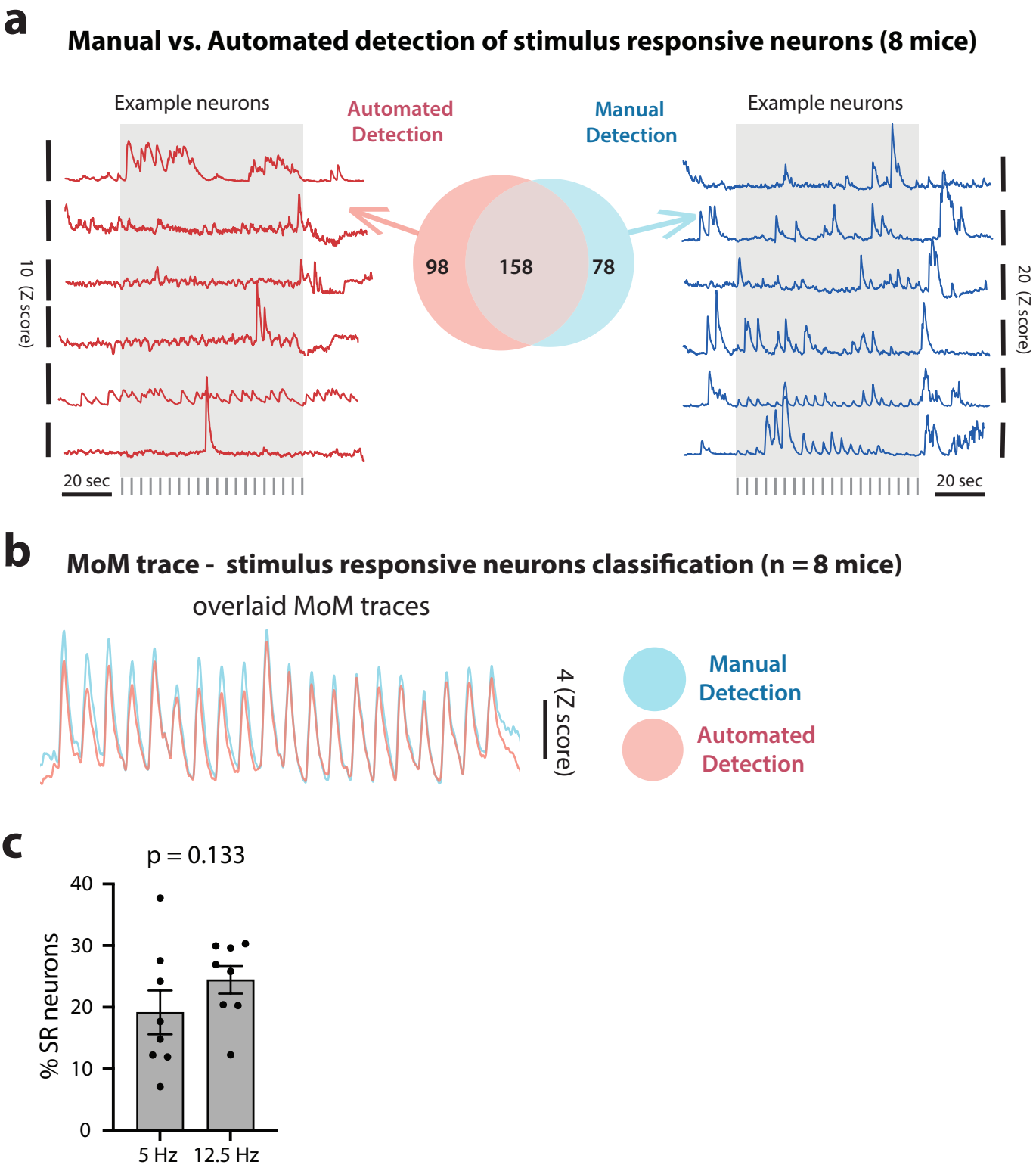

Suppl. Fig 1 (for FIG 1)

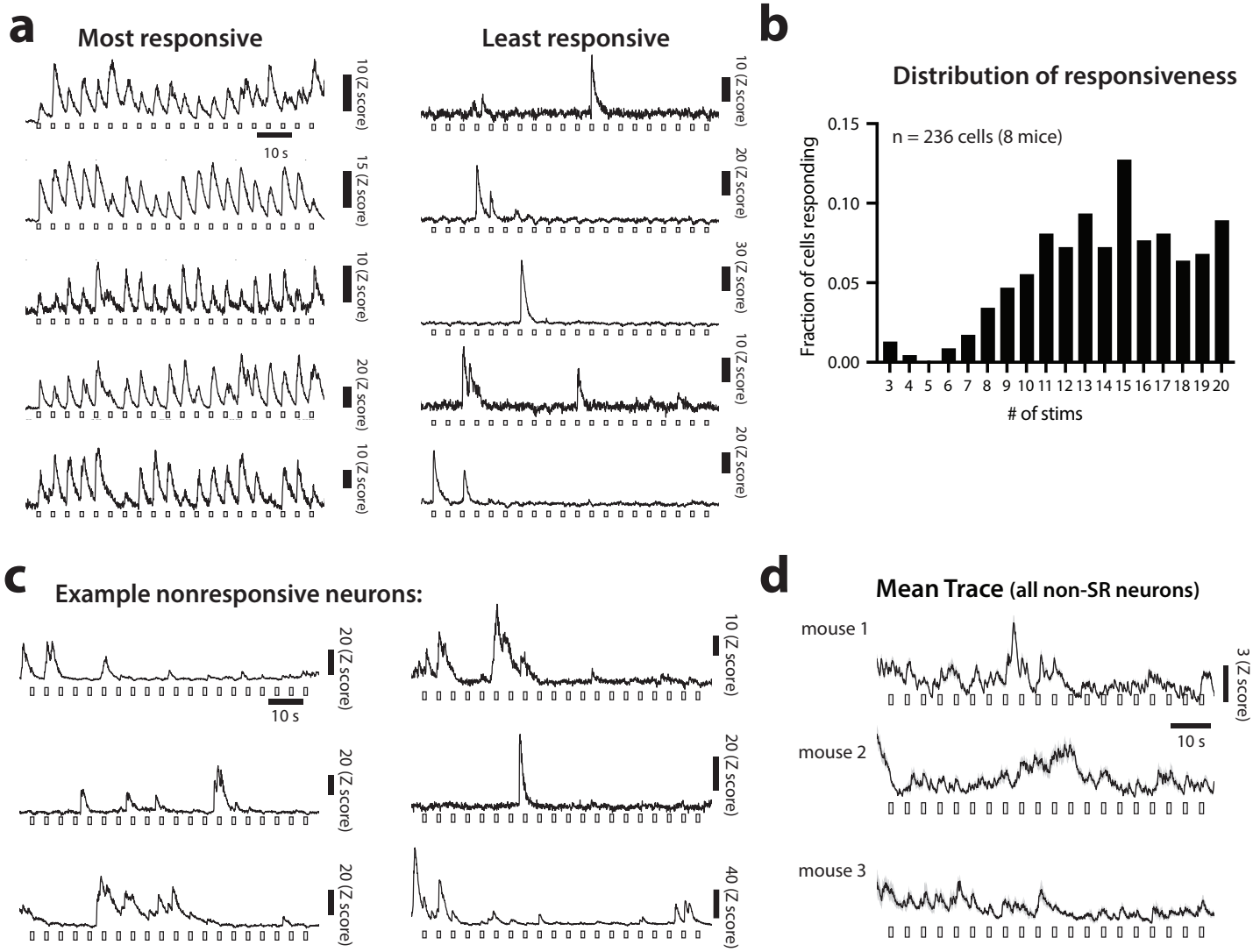

Suppl. Fig 2 (for FIG 1)

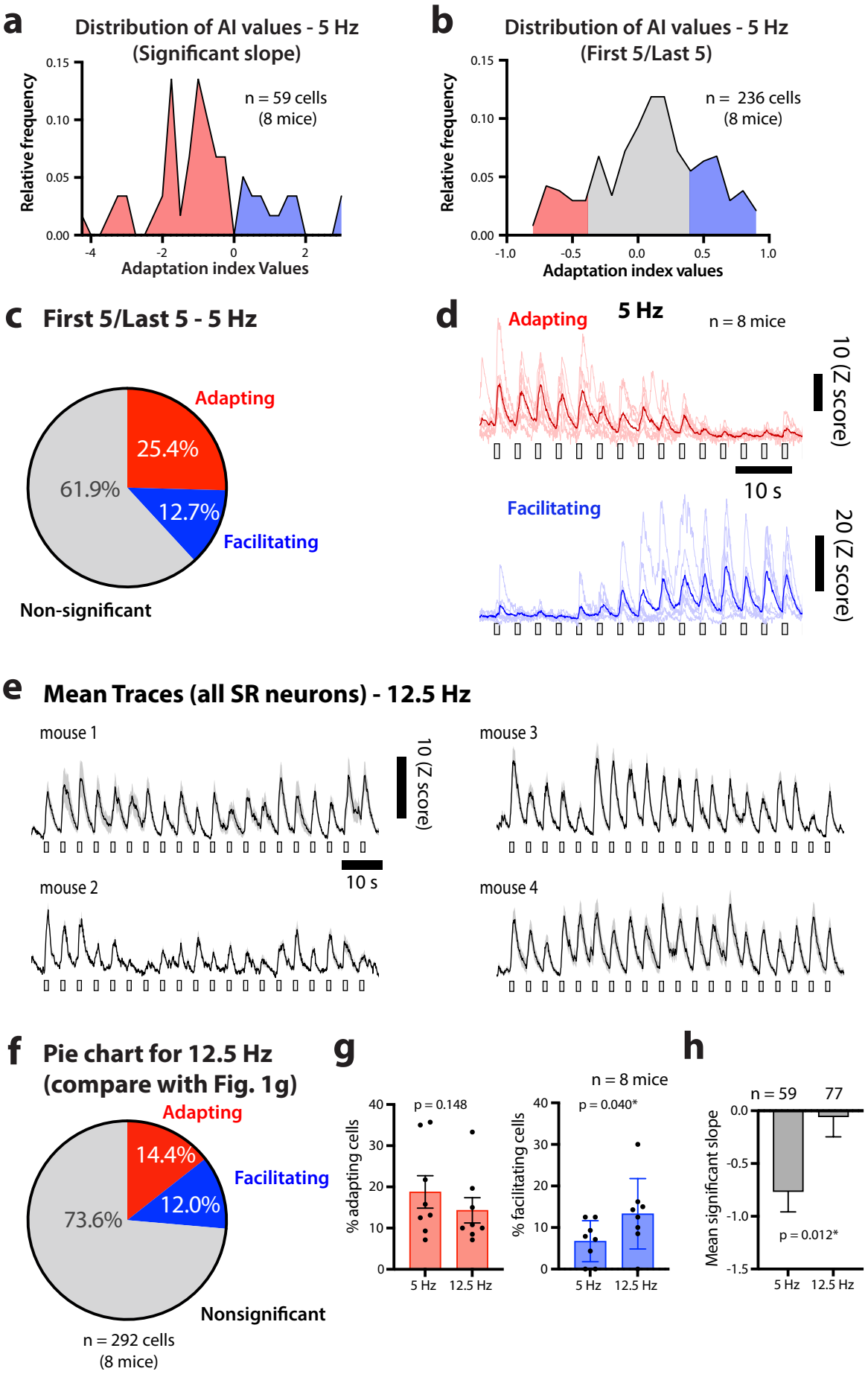

Suppl. Fig. 3 (for FIG. 1)

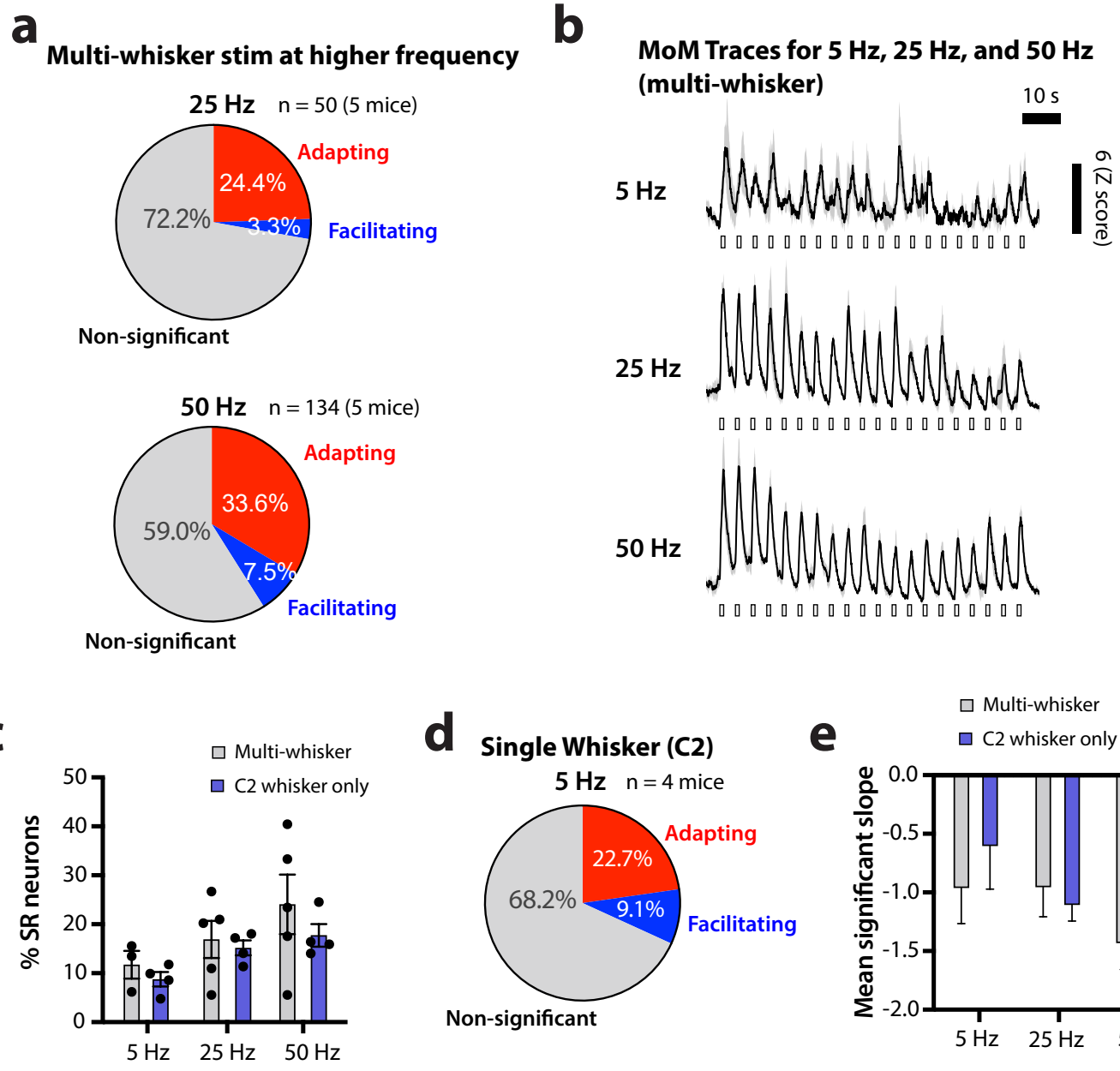

Suppl. Fig. 4 (for FIG. 1)

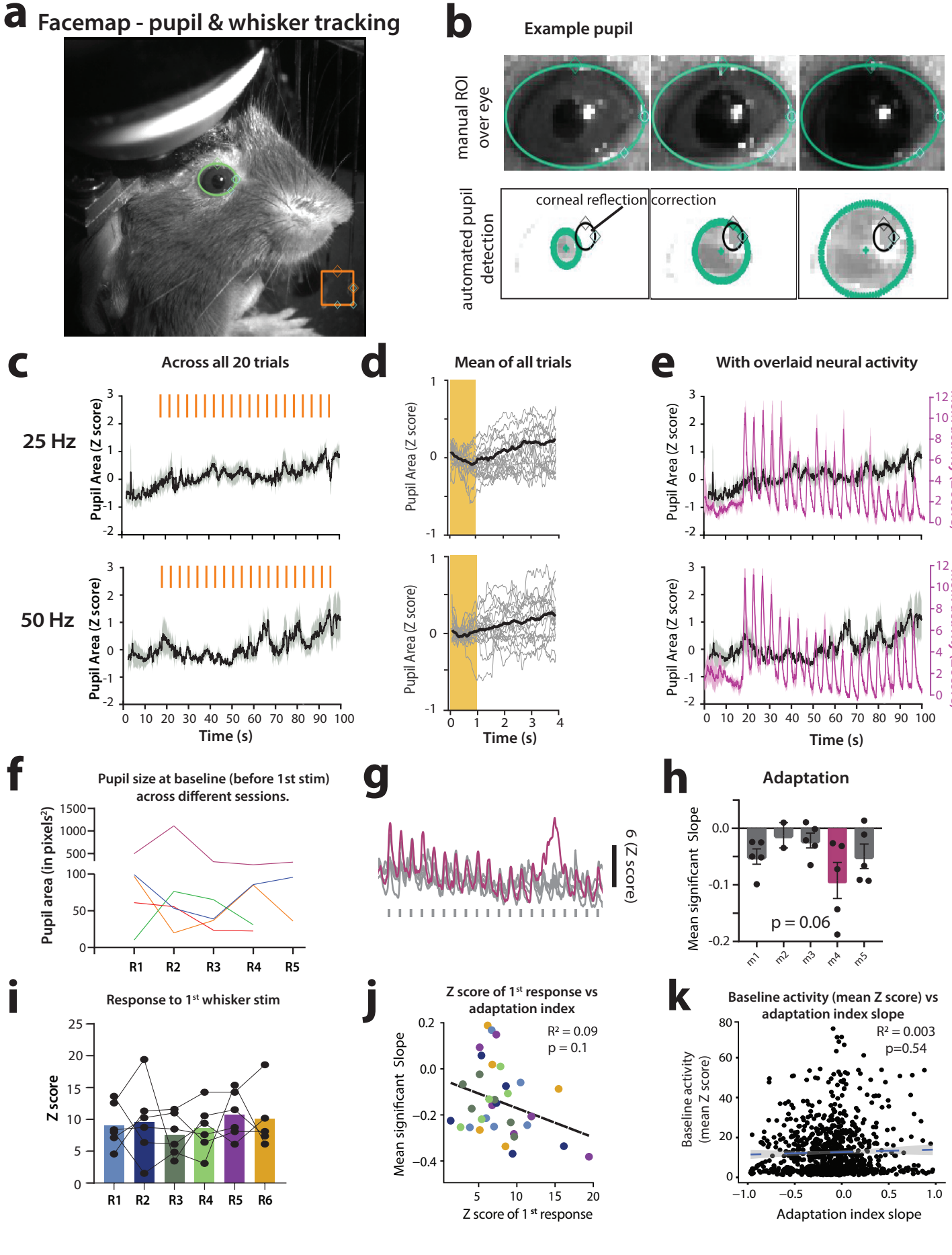

Suppl. Fig. 5 (for FIG. 1)

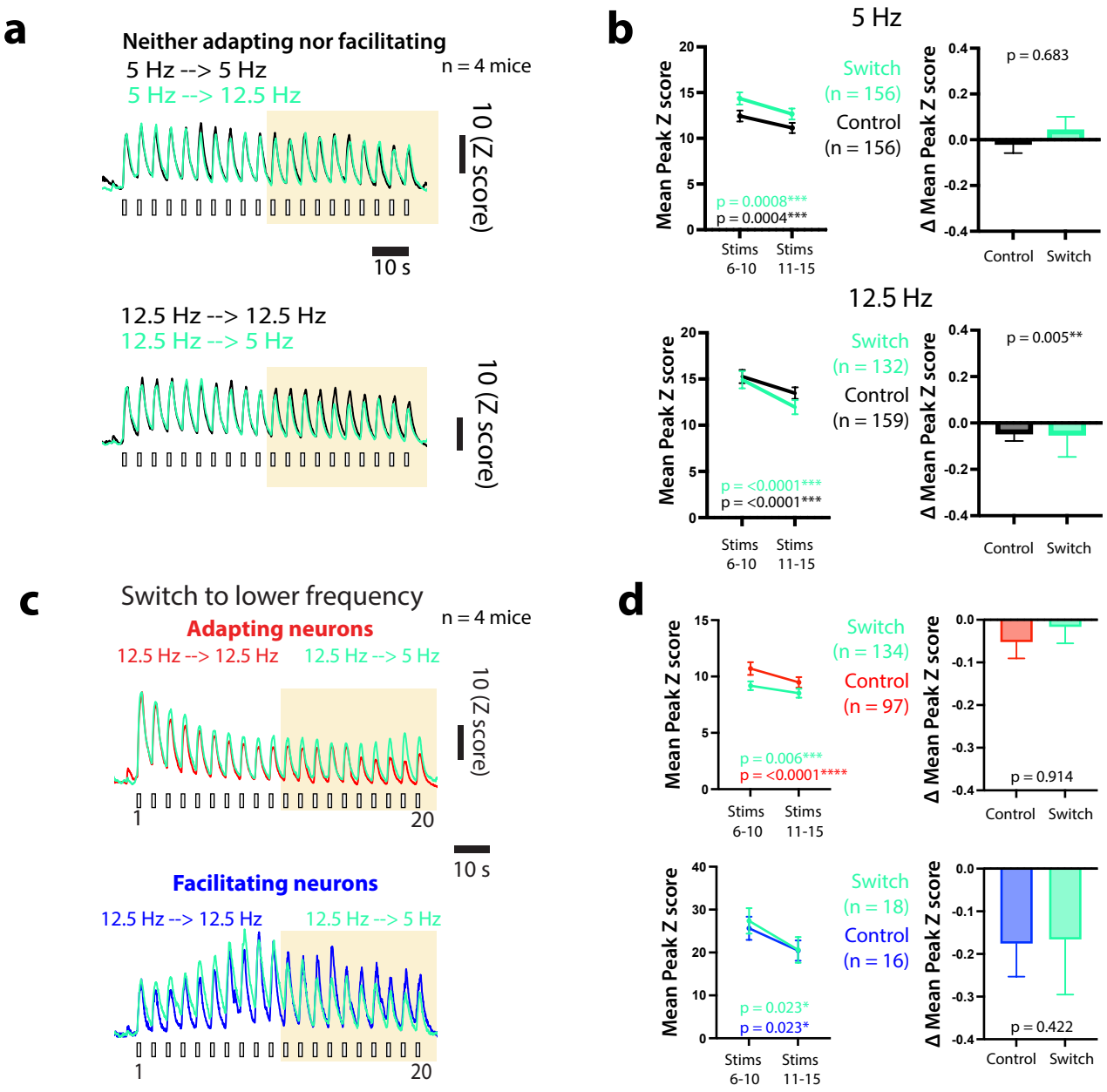

Suppl. Fig. 6 (for FIG.3)

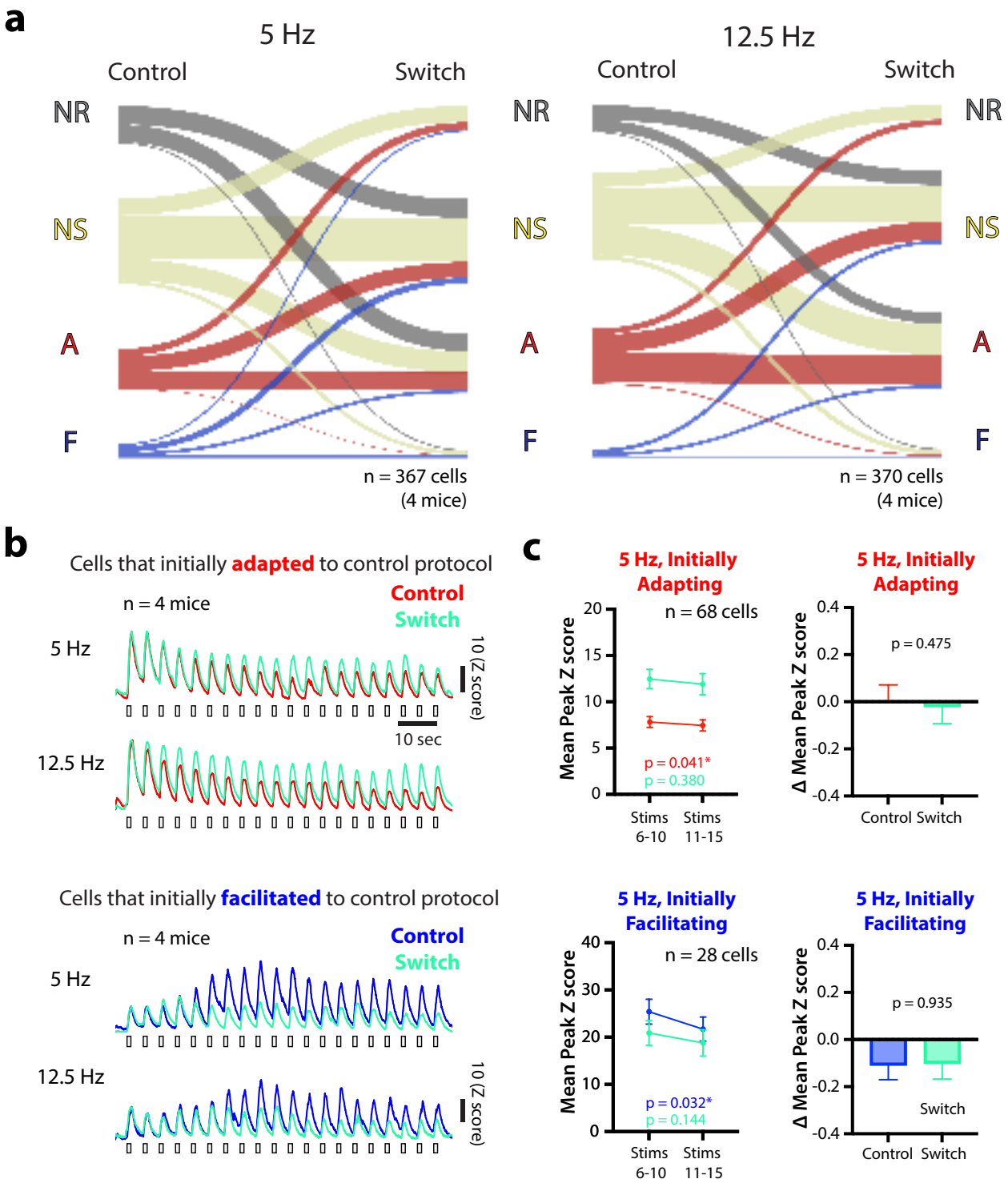

Suppl. Fig. 7 (for FIG.3)

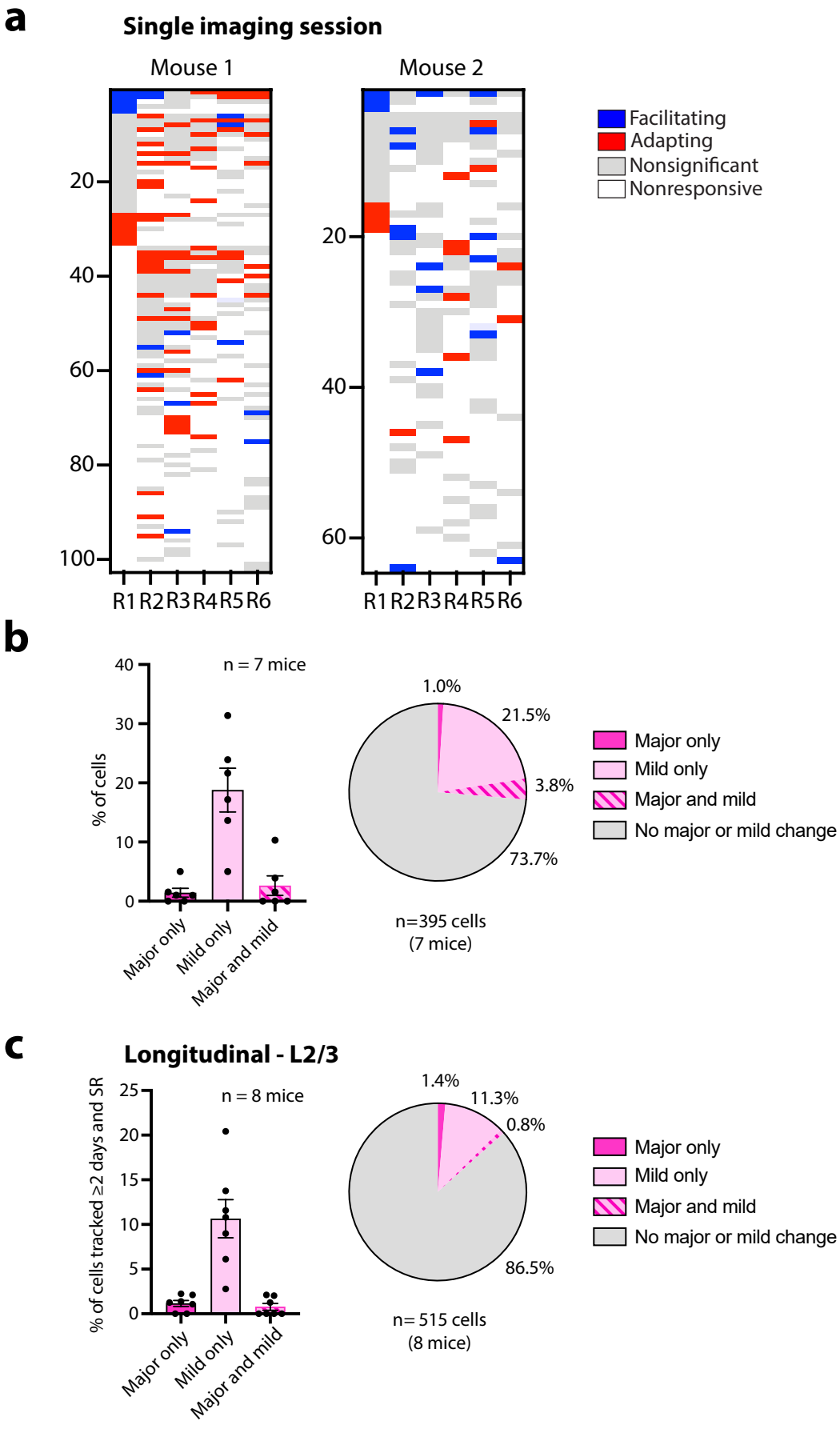

Suppl. Fig. 8 (for FIG. 4 & 5)

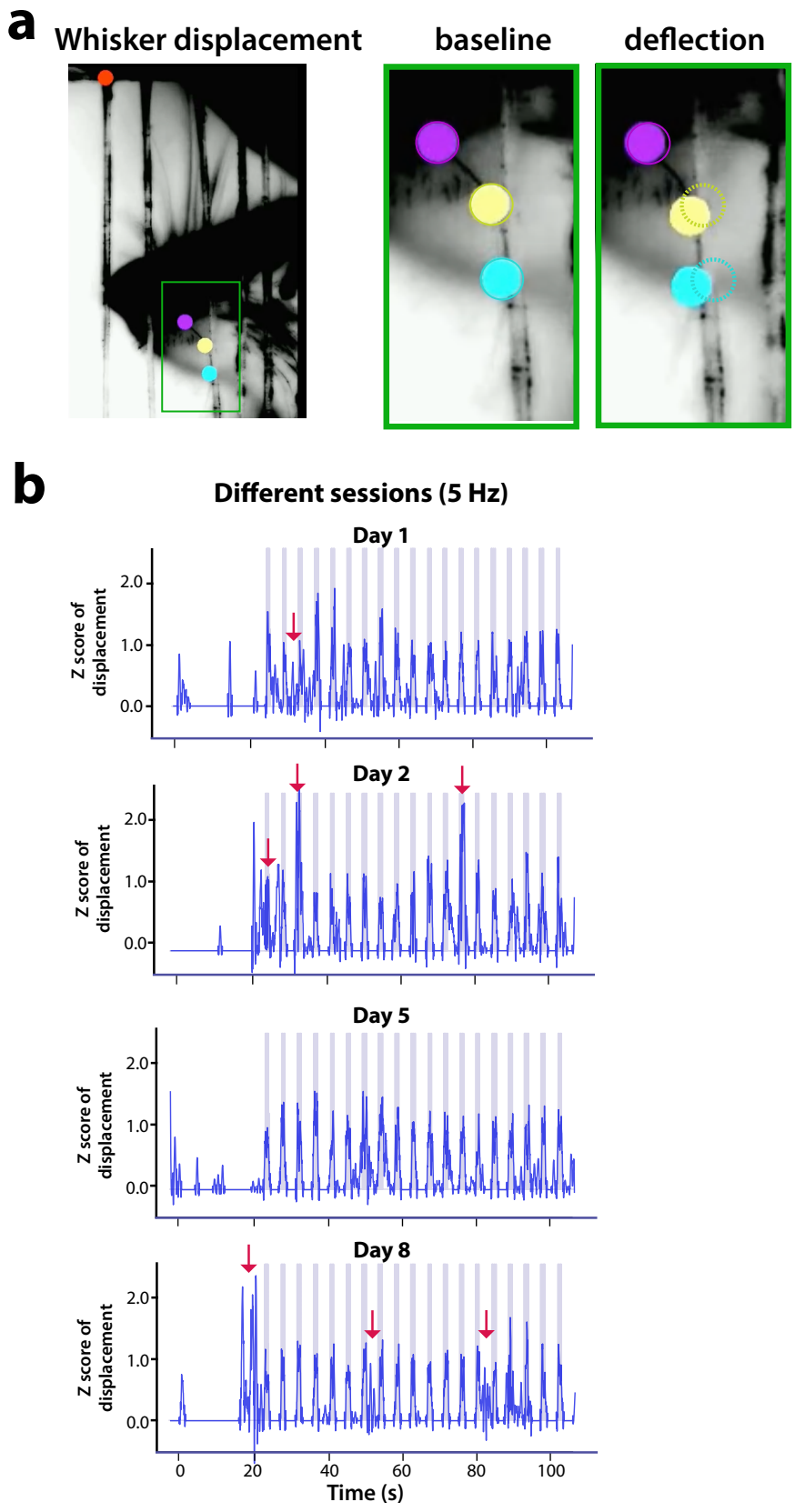

Suppl. Fig.9 (for Fig. 5)

Scnn1a-Cre;Ai162 mice (Layer 4)

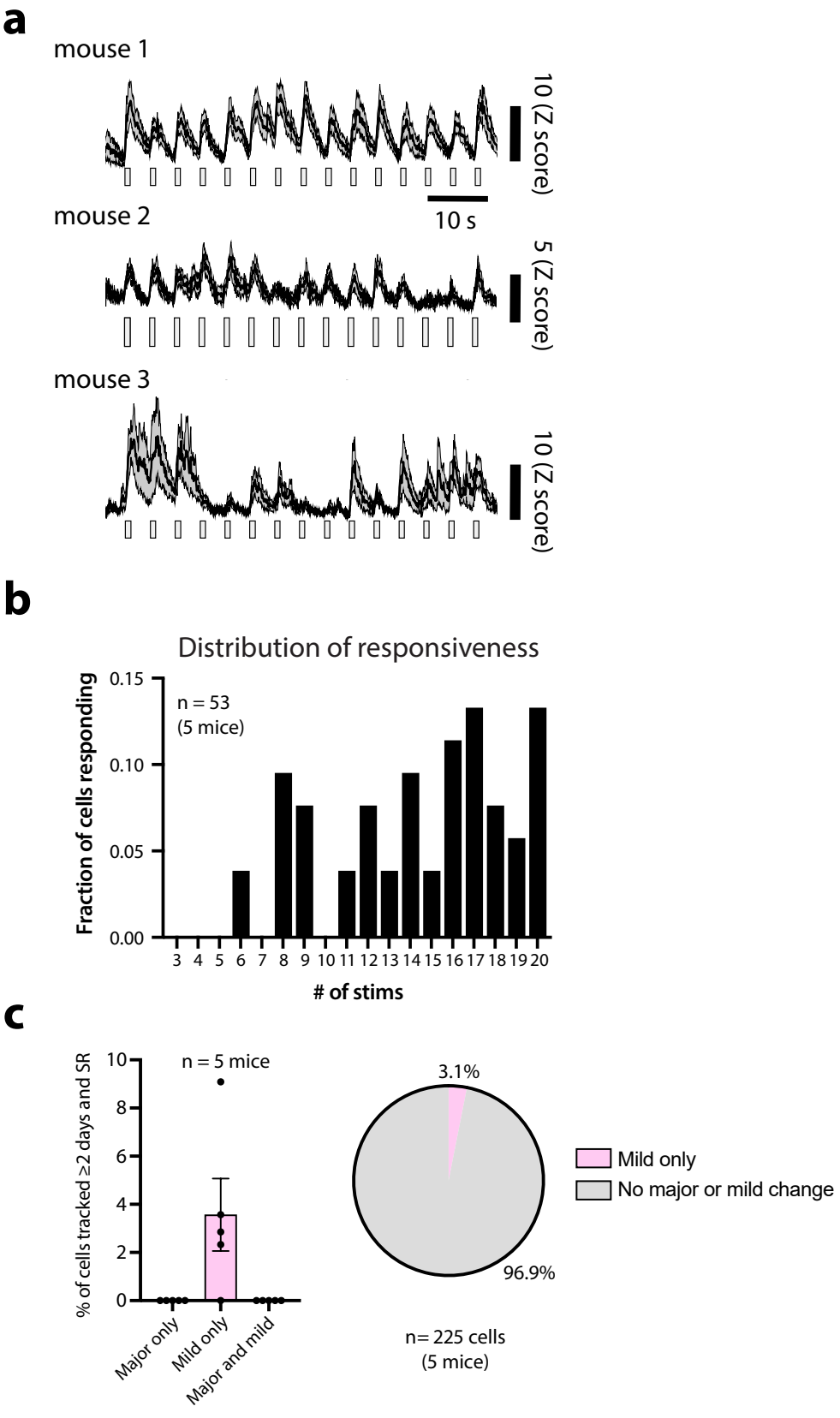

Suppl. Fig.10 (for Fig. 6)

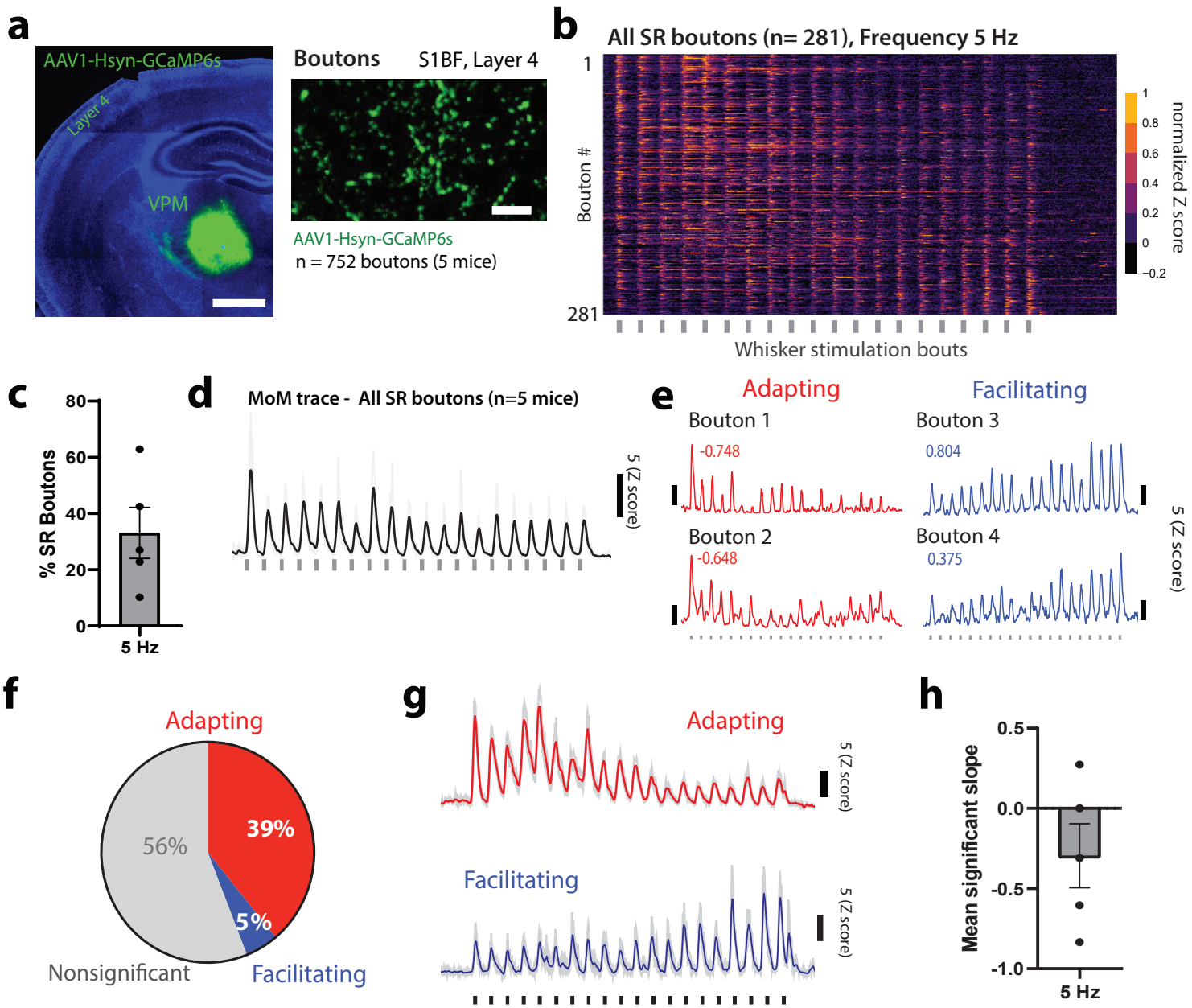
a
AAV1-Hsyn-GCaMP6s
Layer 4
VPM
Boutons
S1BF, Layer 4
AAV1-Hsyn-GCaMP6s
n = 752 boutons (5 mice)
b
All SR boutons (n= 281), Frequency 5 Hz
1
Bouton #
281
normalized Z score
1
0.8
0.6
0.4
0.2
0
−0.2
Whisker stimulation bouts
c
% SR Boutons
80
60
40
20
0
5 Hz
d
MoM trace - All SR boutons (n=5 mice)
5 (Z score)
e
Adapting
Facilitating
Bouton 1
-0.748
Bouton 3
0.804
Bouton 2
-0.648
Bouton 4
0.375
5 (Z score)
f
Adapting
39%
56%
5%
Nonsignificant
Facilitating
g
Adapting
5 (Z score)
Facilitating
5 (Z score)
h
Mean significant slope
0.5
0.0
-0.5
-1.0
5 Hz

Suppl. Fig. 11

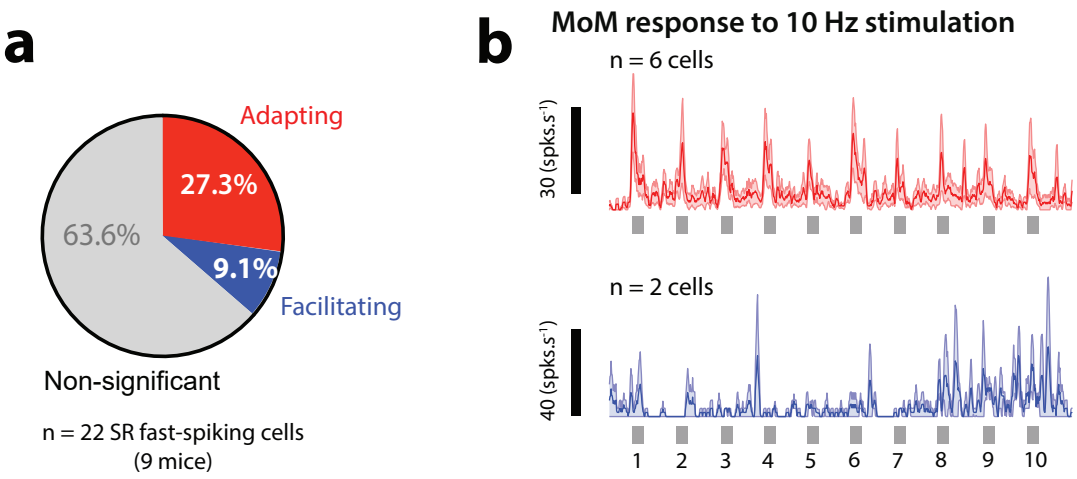

Suppl. Fig.12 (for FIG. 7)